The Compatibility Quotient of the Penrose Kite–Dart Matching Rules and a Three-Chord Signature Realizing It

Sebastian Pardo-Guerra[1], Jonathan Washburn[1], and Elshad Allahyarov[1,2,3,4]

[1]*Recognition Physics Institute, Austin, TX, U.S.A.*
sebas@recognitionphysics.org , jon@recognitionphysics.org
[2]*Institut für Theoretische Physik II: Weiche Materie, Heinrich-Heine Universität Düsseldorf, Germany*
[3]*Theoretical Department, Joint Institute for High Temperatures, Russian Academy of Sciences (IVTAN), Moscow, Russia*
[4]*Department of Physics, Case Western Reserve University, Cleveland, OH, U.S.A.*
elshad.allakhyarov@case.edu

Submitted: Aug 4, 2026; Accepted: TBD; Published: TBD

Abstract. The Penrose kite–dart matching rules are a symmetric relation on the finite set of marked-edge types of the two prototiles. This paper analyzes the rule one side of an edge at a time. We form the Myhill–Nerode quotient of the rule: two half-edge classes are equivalent when they accept the same partners among the fourteen realizable ordered pairings. We prove that the quotient has exactly six classes, realized exactly by an explicit three-chord assignment that agrees with the classical Ammann decoration in its edge-stable content. The assignment's three-chord signature, the relative bar family modulo five and the normalized position of each crossing, takes one value per class, with crossing fractions $\frac{1}{4}$, $\frac{3}{4}$, $\frac{1}{2\varphi^2}$, and $\frac{\varphi}{2}$, where $\varphi = (1+\sqrt{5})/2$. No coarser edge-local datum can separate the classes, and this one separates them exactly. Positional information is essential: the signed count, restricted to the admissible families, depends on the edge vector alone, and the kite-plus-dart rhombus tiles the plane periodically with every count condition satisfied while the matching rule fails at asymptotically half of its interior edges. The dart's short classes are separated from the kite's by the dart's notch chord, invisible to the count, and the decoration divides each long edge in the ratio $\varphi^3 : 1$ and each short edge $3 : 1$. Every entry of the resulting signature table is derived symbolically in $\mathbb{Q}(\sqrt{5})$, and that derivation is the proof. The six classes, their signatures, and the identification with the classical decoration are independently confirmed by computation on a single certified 372-tile patch.

Keywords. Penrose tilings, matching rules, Ammann bars, Myhill–Nerode quotient, compatibility classes, golden ratio, local rules

Mathematics Subject Classifications. 52C23, 52C20, 68Q45

1. Introduction

1.1. The question

The Penrose kite–dart tilings (P2) [Pen74, BG13] are defined by local matching rules. Each edge of the two prototiles carries an arrow decoration, and a tiling by copies of the prototiles is valid when the decorations of the two tiles incident to a shared edge agree [GS87, §10.3].

Every valid tiling is nonperiodic, so the decorated prototiles form an aperiodic set, and the matching rule is the mechanism responsible. Formally, the rule is a symmetric relation on the finite set of marked-edge types of the prototiles. It constrains, for each side of each edge, which marked tiles may occur across that edge.

The one-sided content of the rule is captured by a quotient. Up to orientation-preserving rigid motion, a prototile together with one of its marked edges, directed counterclockwise around the tile, determines one of eight *half-edge classes*, one for each of the four edges of each of the two prototiles. The *partner set* of a class is the set of classes it may legally meet across an edge *in some valid tiling of the plane*, and two classes are declared equivalent when their partner sets coincide. The occurrence requirement is not a technicality: dropping it admits a pairing that no valid tiling contains and collapses the quotient computed below, as Definition C.1 records. This is the Myhill–Nerode equivalence of the rule [Myh57, Ner58, HU79], and the quotient of the eight classes by this equivalence is the *compatibility quotient* of the rule. The quotient is intrinsic to the rule. Its definition mentions no decoration of the tiles.

The question addressed here is whether this quotient can be read from a geometric decoration of the prototiles, that is, from an edge-local datum drawn on the tiles themselves. More precisely, we ask whether some assignment of straight chords to the two prototiles, recorded on each half-edge as the relative chord family and the normalized position of each crossing, realizes the compatibility quotient, and whether a coarser edge-local datum already suffices. The assignment examined here is read off the classical Ammann bar decoration [GS87, §10.6], which is the provenance of the three chord families and the offsets of (2.1); the results themselves are statements about that explicit assignment.

1.2. Prior work

Aperiodic tiling theory has seen substantial recent activity. We refer to the surveys [Tre23, BW23] and recall here only the developments that bear directly on the present paper. The Einstein problem—whether a single shape can tile the plane, but only nonperiodically—was solved by the hat monotile [SMKGS24a] and, in the chiral setting, by the Spectre [SMKGS24b]. The periodic tiling conjecture was disproved in high dimensions [GT24]. Undecidability of tiling questions goes back to Robinson [Rob71], and now reaches very small tile sets: whether three given polygons can tile the plane is undecidable [DL25], and so is monotiling under edge-to-edge matching rules [Sta25].

Matching rules continue to be constructed for new systems, including hierarchical rules obtained from inflation data [WW23]. The new monotiles have been incorporated into the general theory: group-theoretic models [CGGL26], tiling-space topology [BGS25, BGMS25], and explicit diffraction [Soc23, BGMM25]—the hat's quasiperiodicity is governed by the golden mean [Soc23]. The Penrose tilings themselves remain a focal point of current work: patch frequencies [Maz23], lattice-point counting [HL25], frieze patterns [FM26], the substitution–projection interface [HKW25, BH23], and quantitative substitution dynamics [BGG25, MM26, FGM24].

The classical theory underlying the present constructions is recalled in Section 2. Two classical frameworks require explicit scoping. The pentagrid construction of de Bruijn, which encodes a tiling in five superimposed families of parallel lines [dB81], enters only through the certification pipeline of Appendix B. The weak-local-rules framework of Levitov [Lev88] and Socolar [Soc90] is recalled for contrast and is not used in any proof: a tile set admits weak local rules when its tilings are exactly the projections of the tilings of a lifted, decorated tile set satisfying ordinary local rules, and the lifted legality test presupposes a legal lifted structure, so it cannot be run on an arbitrary candidate tiling, in particular not on the candidate tilings considered here. The classical Ammann-bar characterization [GS87, AGS92] motivates the present constructions but is never used as an input. Remark 3.14 records its exact scope. Recent work on the local structure of classical tiling systems bears on the present question from several sides. Bédaride and Fernique prove the non-existence of weak local rules for the $4p$-fold tilings [BF15], and Fernique and Lutfalla characterize the geometrical Penrose tilings by their radius-one patch data (their 1-atlas [FL24]). Fernique and Porrier construct Ammann-bar decorations for octagonal systems [FP24]. Minnick tabulates the bar-to-tile distances of the classical P2 decoration for the empire (forced-tile) problem [Min98]. None of these works computes the P2 compatibility quotient or identifies a drawn decoration realizing it.

The equivalence used here has a well-known one-dimensional ancestor that should be named. Identifying states of a language by their right contexts is the construction behind the Fischer cover of an irreducible sofic shift [Fis75] and behind Krieger's canonical cover [Kri84]; both are standard, and are developed systematically in Lind and Marcus [LM95, Ch. 3]. The compatibility quotient of Definition C.1 is the one-step analogue of that construction for a two-dimensional edge-matching rule, with the right context of a half-edge taken to be its set of legal partners across a single edge. Two consequences of this analogy should be stated plainly, since they bound what is claimed below. First, the covers just cited are constructions for one-dimensional shift spaces and have not, so far as we can determine, been computed for the P2 edge language, which is what makes the present computation worth carrying out rather than quoting. Second, only the *one-step* quotient is computed here. Whether the partition refines under longer right contexts, contexts of a half-edge within a patch of radius $r > 1$, is not addressed, and the six classes of Proposition 4.1 are not claimed to be stable under such refinement. The corresponding hierarchy question is recorded in §6.

Until the quotient is computed, one cannot say how much of a matching rule's content is visible in any edge-local datum. The quotient is the benchmark against which any such datum must be measured. The benchmark is defined for any finite-range edge-matching rule (Definition C.1), including rules with no geometry to draw. The extreme case is a purely color-matching set such as the aperiodic Wang set of Jeandel and Rao [JR21], where the quotient is still defined but the question of a drawn realization does not arise.

1.3. Main results

The results form a hierarchy of detection data, each level strictly finer than the preceding one. The new content is concentrated in part (iii). Parts (i) and (ii) are the structural analysis on which it rests; part (ii) in particular restates a classical criterion rather than establishing a new one (Remark 3.20). The computations in (iii) are finite enumerations over eight classes resting on the classical vertex-star classification. To our knowledge, neither the compatibility quotient of the P2 rule nor a drawn decoration realizing the quotient of any aperiodic matching rule appears in the prior literature. The new content is the quotient, its realization by the three-chord signature, and the separation of the crossing count from the crossing position; the finite enumerations that support these are elementary, and no novelty is claimed for them. §7 states the three in the same terms.

The underlying equivalence is not new, and its ancestry in the covers of a sofic shift is set out in §1.2. The novelty claim is accordingly a report on a literature search, restricted to the one-step quotient, and not an assertion that the computation could not be assembled from the cover literature by a reader who set out to do so.

(i) **The count is rigid, and position is essential.** The signed bar-crossing count of an edge, restricted to the admissible families of Definition 3.1, is determined by the edge vector alone (Lemma 3.15). The restriction is what discards the geometric content: the raw, unrestricted count differs between kite and dart placements (Proposition 3.6). Agreement of the restricted count across a shared edge is therefore vacuous as a detection criterion, and no datum computed from the counts alone can detect the rule: the kite-plus-dart rhombus tiles the plane periodically with all five count conditions satisfied at every edge and the matching rule failing at asymptotically half of them (Propositions 3.16 and 3.17, Figure 3.1).

(ii) **Position detects the rule.** Read through the crossing positions, the classical rule becomes an explicit eight-entry dictionary between the marking on an edge and the positions at which bars meet it (Lemma 3.9), and the count together with the crossing *position* detects the matching rule edge by edge, on arbitrary candidate tilings and on finite patches (Proposition 3.19). This equivalence is a relabeling of the classical rule, not a new local rule (Remark 3.20). Its role in the paper is to put the rule into the positional coordinates on which the quotient analysis of Section 4 runs. The datum carries one bit per edge.

(iii) **The three-chord signature detects compatibility.** The eight half-edge classes, grouped by identical partner sets among the fourteen realizable legal ordered pairings, form exactly six compatibility classes (Proposition 4.1).
The three-chord signature—the relative bar family modulo five and the normalized position of each chord crossing—takes six distinct values, one per class (Theorem 4.3), and is the *coarsest* signature detecting the rule (Remark 4.6), the coarseness holding by the definition of the quotient.
The count cannot supply the separation: on one short-edge vector all four short classes occur, with partner sets of sizes $1, 1, 2, 2$ (Corollary 4.7). What separates the dart's short classes from the kite's is the dart's notch chord, invisible to the count and indispensable for compatibility (Remark 4.8).

> Of the two assertions just combined, only the first has geometric content: coarseness restates the definition of $\sim$, whereas Theorem 4.3, that the drawn signature attains the partition exactly, is what could fail for a given decoration and what the computation establishes. Remark 4.6 makes the separation precise.

The signature fractions are golden-ratio quantities (5.1): the decoration divides each long edge in the ratio $\varphi^3 : 1$ and each short edge in the ratio $3 : 1$. Every entry of the signature table is derived symbolically in $\mathbb{Q}(\sqrt{5})$ (Appendix A), and the six-class quotient, the six signatures, and the two-sided agreement of the measured crossing sets at all 670 interior gluings are corroborated by computation, within stated tolerances, on a single certified 372-tile patch extracted from the Tilings Encyclopedia kite–dart patch [HF] (Appendix B).

1.4. Organization

Section 2 summarizes the Penrose background: candidate decorated tilings, the three-chord assignment, and the geometric facts used below. Section 3 builds the crossing data and proves parts (i) and (ii). Section 4 forms the compatibility quotient and proves part (iii). Section 5 records the golden-ratio content of the signature. Section 6 states the open problems, and Section 7 concludes. Appendix A derives the signature table symbolically. Appendix B describes the computational certification.

Appendix C records the general form of the compatibility quotient together with the elementary and standard material moved out of the main text, from the cyclotomic relation lemma to the uniqueness discussion for the cost function of Remark 5.2.

2. The Penrose Tiling and Its Ammann Bars

This section collects the background used below. The Penrose prototiles, the matching rules, the Robinson decomposition, the vertex-star classification and the classical Ammann-bar characterization are quoted from the literature and cited at each point of use; their proofs are not repeated. Two constructions are introduced here and used throughout: the notion of a candidate decorated tiling (Definition 2.1), which allows bar data to be read on tilings that violate the matching rules, and the explicit three-chord assignment $\mathcal{A}$ of (2.1). The remaining material is elementary but is nonetheless proved rather than cited, because we have not located it in the form needed: the edge-vector inventory (Lemma 2.10), the count of families crossing an edge (Lemma 2.11), and the crossing vectors of Table 2.1.

2.1. Standing assumptions and scope conventions

To prevent hidden hypotheses from being used implicitly, we adopt the following standing conventions.

(a) **Penrose model.** Unless stated otherwise, "Penrose tiling" means the P2 (dart–kite) system with the standard edge decorations and Ammann bars as in §2.2.

(b) **Candidate vs. valid.** "Candidate decorated tiling" means Definition 2.1 (decorations are present but may violate matching rules). Statements that require validity explicitly assume matching rules (or invoke Proposition 3.19).

(c) **Graph conventions.** All crossing data are functions of a directed tile edge, that is of an ordered pair of adjacent tiling vertices together with a side. The underlying graph is recorded in Definition 2.4 and used only for the connectedness argument in the proof of Lemma 2.10.

(d) **Orientation normalization.** In an edge-to-edge tiling by darts and kites all edge vectors lie in a single rigid set of ten unordered $\{v, -v\}$ pairs (Lemma 2.10). Every candidate tiling is assumed rotated so that this set is the reference set $\mathcal{E}$ of that lemma. All statements are invariant under the choice, and the admissible index sets $S(v - u)$ and the family indexing below presuppose it.

(e) **No cut-and-project formalism.** All statements are proved directly from the bar geometry, not through the cut-and-project description of aperiodic tilings as slices of higher-dimensional lattices.
The pentagrid enters only through the certification pipeline (Appendix B and Remark 4.9).

2.2. Prototiles, matching rules, and Ammann bars

We work with the dart–kite (P2) formulation [Pen74, BG13], where each prototile is a quadrilateral with edges of length 1 (short) and $\varphi = (1 + \sqrt{5})/2$ (long). Each prototile is cut by the classical Robinson decomposition [BG13, Ch. 6], [GS87, §10.3] into two *Robinson half-tiles*, the pieces on which inflation acts with linear factor φ, where $\varphi^2 = \varphi + 1$ and $\varphi^3 = 2\varphi + 1$.

Each prototile edge carries arrow decorations (equivalently Conway's arcs [GS87, §10.3]) enforcing the *matching rules*: two tiles may share an edge only if their decorations agree, and these local constraints forbid periodic arrangements and enforce global aperiodicity [Pen74].

For a valid tiling, the decorations also determine five families of *Ammann bars*—sets of parallel straight lines crossing the tiling continuously [GS87, BG13]. Each family has a fixed direction (one of five related by $72°$ rotations, illustrated in Figure 2.1), and the perpendicular spacings between consecutive bars form a Fibonacci quasiperiodic sequence [BG13, Ch. 4] with short gap S and long gap $L = \varphi\, S$, the two gap types alternating according to the Fibonacci word (the two-letter sequence generated by the replacements $L \mapsto LS$ and $S \mapsto L$).

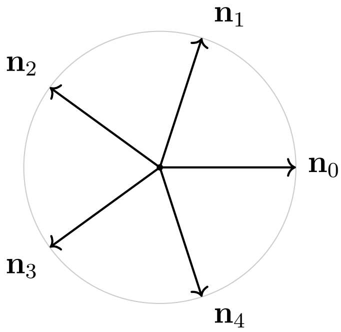

Figure 2.1: The five Ammann bar families for Penrose P2 are indexed by unit normals $\mathbf{n}_k$ related by $72°$ rotation. A "bar family direction" means the direction of the bar lines. Its normal $\mathbf{n}_k$ is used to assign signed crossing numbers to directed edges.

The classical Ammann-bar characterization [BG13, §6.2], [GS87, §10.6] states that the matching rules are satisfied if and only if the Ammann bars form continuous straight lines, bars not terminating inside the tiling. Definition 2.3 makes the notion precise, and Remark 3.14 records the exact scope in which we use this characterization.

2.3. Candidate decorated tilings and local bar data

The following definitions make bar data meaningful for *candidate* tilings that may violate the matching rules—providing the vocabulary needed for Proposition 3.19.

Definition 2.1 (Candidate decorated Penrose tiling)**.** A *candidate (decorated) Penrose tiling* is an edge-to-edge tiling (tiles meet only full edge against full edge) $\mathcal{T}$ of $\mathbb{R}^2$ by dart and kite prototiles, where each tile carries the standard Penrose edge decorations (arrows/arcs), but adjacent tiles are not assumed to satisfy the matching rules (decorations on a shared edge may disagree). By Remark 2.2 the decoration of a tile is determined by the region it occupies, so nothing is being chosen here: a candidate decorated Penrose tiling is precisely an edge-to-edge kite-and-dart tiling of the plane, and validity is a property of the underlying undecorated tiling.

The longer name is retained for emphasis rather than for content. The results of §3 read bar data off tilings on which the matching rules are not assumed, that being the whole point of Lemma 3.9(iii) and of the witnesses of Proposition 3.16, and the word "candidate" carries that qualification, which would otherwise have to be restated in each hypothesis. The quotient of §4 does by contrast quantify over valid tilings.

Remark 2.2 (The P2 decoration is determined by the tile's placement)*.* It is worth stating explicitly, because the phrase "candidate decorated tiling" can suggest otherwise, that there is exactly one decorated tile per placed region. Both prototiles are mirror-symmetric about the axis joining their two axial vertices, and *their decorations are invariant under that reflection*, so a region determines its decoration. There is no binary choice per tile, and hence no "decoration freedom".

The verification is recorded in Appendix C, family by family, as Remark C.5.

One nuance deserves emphasis, as it is a frequent source of confusion. Chirality does appear one level down: the Robinson half-tiles are chiral, and each of them admits two mirror-image subdivisions, the choice between them being exactly what the matching rules determine. A reader working with half-tiles therefore does face a binary choice per tile. A reader working with whole kites and darts, as we do throughout, does not.

Definition 2.3 (Local and global Ammann bars)**.** Fix one of the five Ammann bar family directions, specified by a unit normal vector $\mathbf{n}$. A *chord assignment* for family $\mathbf{n}$ gives each decorated prototile a finite collection of straight segments inside the tile, all lying on lines with normal $\mathbf{n}$ (equivalently, all parallel to the bar direction) [GS87, BG13]. These are the *local bar segments* of the tile. Given a chord assignment $\mathcal{C}$ and a candidate tiling $\mathcal{T}$, let $\mathcal{B}_{\mathbf{n}}^{\mathcal{C}}(\mathcal{T})$ denote the set of connected components of the union of all such segments over tiles of $\mathcal{T}$. Its elements are the (possibly broken) *Ammann bars* of family $\mathbf{n}$, and the family is *continuous* if every component is an entire straight line in $\mathbb{R}^2$ (equivalently, has no endpoints in the interior of $\mathbb{R}^2$).

Two chord assignments occur in this paper and *must not be conflated*.

(a) The *classical quasigrid* assignment $\mathcal{Q}$, which is the standard Ammann decoration of the kite and dart as it appears in the sources cited above.
Continuity of all five families of $\mathcal{Q}$ is the condition appearing in the classical Ammann-bar characterization.

(b) The *three-chord* assignment $\mathcal{A}$ given explicitly by the offsets (2.1), from which the signed count Δ and the crossing position τ are computed (Definition 3.1, Definition 3.7). We write $\mathcal{B}_{\mathbf{n}}^{\mathcal{A}}$.

Thus local bar data are readable tile-by-tile on any candidate tiling, with no global validity assumption. The chords of $\mathcal{A}$ are among those drawn in the published figures of $\mathcal{Q}$, and not all of them; that comparison is empirical, in the sense made precise in Remark 2.7. By contrast, $\mathcal{B}_{\mathbf{n}}^{\mathcal{A}}$ is *never* continuous, not even on a valid tiling: it has a genuine gap at every dart notch (Remark 2.9), a statement about $\mathcal{A}$ alone.

The published sources present $\mathcal{Q}$ only through figures of the decorated prototiles with the bars drawn extended through neighboring tiles, which does not determine a unique chord assignment. We therefore use $\mathcal{Q}$ below only as a label for the classical decoration, never as an object of computation.

The candidate tiling and its bar data live on a natural combinatorial structure: the tiling's vertices, joined by the tile edges, form the following graph.

Definition 2.4 (Tiling adjacency graph)**.** Let $\mathcal{T}$ be a Penrose tiling with vertex set V and edge set E. The *tiling adjacency graph* is $G_{\mathcal{T}} = (V, E)$, where a pair of tiling vertices $u, v \in V$ forms an edge, $(u, v) \in E$, exactly when u and v are the two endpoints of a common tile edge.

2.4. Geometric properties of Ammann bars

The following properties of Penrose P2 decorations and Ammann bars are used in §3. See Baake–Grimm [BG13, Ch. 6] for concrete conventions.

Remark 2.5 (Transversality and parity). Property (i) is classical decoration data [BG13, §5.7], [GS87, §10.6], [AGS92]. The rest follows from it, from the shapes of the two prototiles, and from the definition of a chord.

(i) No bar of a given family is parallel to any tile edge, and no bar passes through a tiling vertex. (The angles occurring between a bar and an edge are $18°$, $54°$ and $90°$. The perpendicular case is not excluded, and a short edge $\pm\mathbf{n}_k$ is crossed by family k, whose bars are perpendicular to it. Family k need not be the *only* family crossing that edge. See Remark 2.8.)

(ii) Each tile edge is crossed by *at most one* local bar chord of any one family. (A *chord* is a connected component of $L \cap t$ for L a bar line of the family. On a non-convex prototile a single line may contribute more than one chord.)

(iii) For each tile t and each bar family $\mathbf{n}$, each chord meets exactly two edges of ∂t, entering through one and leaving through the other. Hence the number of edges of ∂t crossed by family-$\mathbf{n}$ chords is *even*.

(iv) The two edges met by a single chord receive opposite *raw* signs.

By (ii) the crossing datum of Definition 3.1 is single-valued, hence the position τ of Definition 3.7 well defined.

Definition 2.6 (Reference prototiles and the three-chord assignment $\mathcal{A}$)**.** Place the reference prototiles with counterclockwise boundary X, Z', Y, Z and $\zeta = e^{2\pi i/5}$:

kite: $X = 0,\ Z' = 1+\zeta^4,\ Y = \varphi,\ Z = 1+\zeta,$ dart: $X = 0,\ Z' = -\zeta,\ Y = 1,\ Z = -\zeta^4.$

Traversing the boundary counterclockwise from X, the four edges of the kite (respectively dart) are labeled $\mathsf{K}0, \dots, \mathsf{K}3$ (respectively $\mathsf{D}0, \dots, \mathsf{D}3$).

Each prototile carries one chord line in each of three bar families, at the following offsets,

$$\text{kite: } \mathbf{n}_0\cdot x = \mathbf{n}_1\cdot x = \mathbf{n}_4\cdot x = \tfrac{1}{4}, \qquad \text{dart: } \mathbf{n}_1\cdot x = \mathbf{n}_4\cdot x = -\tfrac{3}{4},\ \ \mathbf{n}_0\cdot x = \tfrac{2-\sqrt{5}}{4}, \tag{2.1}$$

and we write $\mathcal{A}$ for the resulting assignment. The name counts chord *lines*: the dart's family-0 line meets the dart in two disjoint chords (Remark 2.8), so the dart carries four chord segments to the kite's three. The offsets are justified a posteriori. The kite's three lines are those of the classical decoration (Remark 2.7), and within the three-chord ansatz the dart's offsets are then forced by cross-edge agreement, proved as Proposition 3.10.

Remark 2.7 ($\mathcal{A}$ versus the classical Ammann decoration). The assignment $\mathcal{A}$ is not an arbitrary choice of three chords. Its relation to the classical Ammann decoration is established in two steps. First, every chord of $\mathcal{A}$ lies on a line of the recovered five-family grid. On the certified patch the bar lines are recovered as the strip boundaries of the pentagrid index: a straight five-family grid whose spacings are the two classical values in Fibonacci-word order. De Bruijn's duality [dB81] is stated for the rhombus (P3) tilings, and the P2 correspondence is not constructed here, so the identification of the recovered grid with the classical Ammann bars shares the empirical status declared at the end of this remark. On the recovered grid, every tile is crossed at least at the chords of $\mathcal{A}$ (Remark 4.9, Appendix B). Second, no further classical crossing is stable. The crossings present at every occurrence of a half-edge class are exactly the chords of $\mathcal{A}$, the remaining ones being neighborhood-dependent, such as the notch-line continuation across the kite's short edges (Remark 4.9). As per-tile chord assignments, therefore, the classical Ammann decoration and $\mathcal{A}$ have the same stable content, and it is this stable content that the signature of Definition 4.2 reads. The assignment $\mathcal{A}$ is used as the object of computation because it is explicit by (2.1).

The status of this remark should be stated exactly. Because the sources define $\mathcal{Q}$ only through figures (Definition 2.3), the identification of $\mathcal{A}$ with the stable part of the classical decoration is an empirical statement, verified on the single certified patch, not a theorem about an abstractly defined $\mathcal{Q}$. It is offered as the historical provenance of $\mathcal{A}$ and nothing more. Because it is empirical, no claim of the form "the classical Ammann decoration realizes the quotient" is made anywhere in this paper: the title, the abstract and every theorem statement refer to the three-chord signature of $\mathcal{A}$, and the word "Ammann" is reserved for the classical bars, chords and decoration themselves.

No proof in this paper takes input from this remark: every theorem below is a statement about $\mathcal{A}$ itself, which is completely defined by (2.1).

Remark 2.8 (The crossing patterns, and why chords rather than lines must be counted). The dart's family-0 offset $\frac{2-\sqrt{5}}{4} = -0.0590\ldots$ lies strictly between the reflex vertex X, at $\mathbf{n}_0$-coordinate 0, and the wings Z', Z, at $-\cos 72°$. That line therefore meets all four dart edges, cutting the wings in two separate chords, and the crossing patterns are

$$\text{kite: } 2,1,1,2, \qquad \text{dart: } 2,2,2,2. \tag{2.2}$$

The kite pattern is consistent with the signed crossing vectors of Remark 2.13. Listed in the boundary order $\mathsf{K}0,\ldots,\mathsf{K}3$ and $\mathsf{D}0,\ldots,\mathsf{D}3$ of Definition 2.6, the dart's pattern $2,2,2,2$ sums to eight chord incidences, two more than the six that three chords each meeting two edges would give: its three lines carry four chords. Since one line may contribute two chords, (iii) is stated per chord (Remark C.3).

The patterns (2.2) are the input to Proposition 3.6, which reads off them that the raw count fails to represent the edge vector at the dart's short edges.

Remark 2.9 (The short-edge asymmetry, and why the admissibility restriction removes it). A kite short edge is met by *one* chord (the perpendicular family, at $\tau \in \{\frac{1}{4}, \frac{3}{4}\}$), a dart short edge by *two*: that family and the family-0 notch chord, at $\tau \in \{\frac{3-\sqrt{5}}{4}, \frac{1+\sqrt{5}}{4}\}$.

In legal Penrose tilings a dart short edge has only kite partners by Lemma 3.4*(i)*, so raw chord counts differ across every dart short edge of a *legal* tiling. The notch chord is nevertheless inadmissible: $\mathbf{n}_0$ is not in the admissible index set of a short edge $\pm\mathbf{n}_k$ with $k \neq 0$, and the dart's two short edges have perpendicular families $\mathbf{n}_1$ and $\mathbf{n}_4$. So Definition 3.1 ignores it, and the tile-side values on a short edge are the same for a kite as for a dart, which Lemma 3.15 verifies at every edge vector and placement. The notch chord cannot be included in the count under any convention (Remark 3.2*(i)*).

Consequently (2.1) does not realize the five families as complete straight lines. The dart's family-0 line is interrupted at the notch: the tiles on the dart's two *short* edges—kites, by the legal pairings $\mathsf{K}2|\mathsf{D}0$ and $\mathsf{K}1|\mathsf{D}3$—carry, in the world frame, chords in families $\{1,2,3\}$ and

$\{2,3,4\}$ only, so the gap, of length $\frac{3-\sqrt{5}}{2}\sin 72^\circ \approx 0.3633$, occurs at every dart notch of every valid tiling. Thus (2.1) is, within the three-chord ansatz and given the kite's three lines, the unique assignment whose *admissible crossings* agree across every shared edge of a valid tiling (proved as Proposition 3.10). The chords themselves agree at only two of the six realizable ordered short-edge pairings, the four dart–kite pairings lacking a partner for the notch chord. Agreement of admissible crossings is strictly weaker than completeness of the lines, since a line may pass through a tile that draws no chord on it.

Two elementary points, that the parity bound in Remark 2.5(iii) must be stated per chord rather than per family, and that the P3 correspondence between bar families and edge-direction classes has no P2 analogue, are recorded in Appendix C.

Lemma 2.10 (Edge vectors of a candidate tiling)**.** *Let $\mathcal{T}$ be a candidate decorated Penrose tiling, normalized so that some edge vector is $\mathbf{n}_0$. Then every edge vector of $\mathcal{T}$ lies in the twenty-element set*

$$\mathcal{E} := \{\pm\mathbf{n}_k : 0 \leqslant k \leqslant 4\} \;\cup\; \{\pm(\mathbf{n}_j + \mathbf{n}_{j+1}) : 0 \leqslant j \leqslant 4\},$$

the two subsets consisting of the short and the long edge vectors respectively, ten of each length, ten unordered pairs $\{v, -v\}$ of edge vectors in all (the twenty vectors span only the five line directions $36^\circ k \bmod 180^\circ$, each carried by one short and one long pair).

Proof. Definition 2.1 permits arbitrary orientations. Each prototile has interior angles that are integer multiples of 36° and two edges of each length 1 and φ, so its edge directions lie in one coset of the group generated by 36° rotations. Edge-to-edge adjacency propagates the coset, connectedness of $G_{\mathcal{T}}$—any two tiling vertices being joined by a chain of adjacent tiles—makes it global, and the normalization fixes it to the ten multiples of 36°. A short edge in one of these directions is $\pm\mathbf{n}_k$, and a long edge is φ times a unit vector in one of them, with $|\mathbf{n}_j + \mathbf{n}_{j+1}| = 2\cos 36^\circ = \varphi$ and $\mathbf{n}_j + \mathbf{n}_{j+1}$ bisecting the directions of $\mathbf{n}_j$ and $\mathbf{n}_{j+1}$. □

The relations among the five bar directions used below are recorded in Lemma C.2 (Appendix C): the integer relation module of $\mathbf{n}_0, \ldots, \mathbf{n}_4$ is generated by $(1,1,1,1,1)$, a standard cyclotomic fact [Was97].

Remark C.4 shows that P2 admits no rule assigning one bar family to each edge-direction class, so the support of the crossing vector must be pinned down some other way. The lemma below does this arithmetically, bounding the support of any $\{-1,0,+1\}$-representation of an edge vector below and thereby making the *minimal-support representative* used in Definition 3.1 well defined. That the bar geometry realizes that representative is a separate, geometric statement, proved by enumeration in Lemma 3.15.

Lemma 2.11 (Support of a signed representation of a P2 edge vector)**.** *Let $u \to v$ be an edge of a Penrose P2 tiling, let $\Delta_{\mathbf{n}_k}(u \to v) \in \{-1,0,+1\}$ satisfy $v - u = \sum_k \Delta_{\mathbf{n}_k}(u \to v)\,\mathbf{n}_k$, and let s denote the number of nonzero values.*

(i) If $\{u, v\}$ is a long edge then $s \geqslant 2$, for every *such Δ.*
(ii) The minimum of s over all admissible Δ is 1 for a short edge and 2 for a long edge.

In particular, no $\{-1,0,+1\}$-representation of a long edge vector has support 1.

Proof. (i): as $|\mathbf{n}_k| = 1$ and the values lie in $\{-1, 0, +1\}$, the triangle inequality gives $|v-u| \leqslant s$. A long edge has $|v - u| = \varphi > 1$ and s is an integer. (ii): by Lemma 2.10 a short edge is $\pm\mathbf{n}_k$ for exactly one k, attaining $s = 1$, and a long edge is $\pm(\mathbf{n}_j + \mathbf{n}_{j+1})$, attaining $s = 2$, minimal by (i). Neither part uses the bar decoration. □

Remark 2.12 (The support size is not determined by the reconstruction equation). Part (ii) needs the bar geometry, since $v-u = \sum_k \Delta_{\mathbf{n}_k}\mathbf{n}_k$ does not determine Δ: by Lemma C.2 two solutions differ by a multiple of $(1,1,1,1,1)$, and that shift can keep all five entries inside $\{-1, 0, +1\}$ while changing the support. Each of the ten unordered edge-vector pairs of Lemma 2.10 has *exactly two* admissible Δ, of *complementary* supports, since if Δ and $\Delta - (1,1,1,1,1)$ both lie in $\{-1,0,+1\}^5$ then the entries of Δ lie in $\{0,1\}$ and those of the shift in $\{-1,0\}$, exactly one of the two nonzero in each coordinate. This lets the ς-invariance argument of Remark 3.18 run without knowing which representative the geometry realizes. For the kite edge of Remark 2.13 in direction $324°$ the two are $(1,0,0,0,1)$ and $(0,-1,-1,-1,0)$, of supports 2 and 3. For the short edge in direction $72°$, $(0,1,0,0,0)$ and $(-1,0,-1,-1,-1)$, of supports 1 and 4.

Which of the two the *raw* count realizes, and the fact that at the dart's short edges it realizes neither, is the content of Proposition 3.6; that third possibility is what forces the admissibility restriction of Definition 3.1.

Remark 2.13 (Consistency of the counts with even parity). On the reference kite of Definition 2.6, with edges taken counterclockwise, the crossing vectors are

$$(1,0,0,0,1), \quad (0,1,0,0,0), \quad (0,0,0,0,-1), \quad (-1,-1,0,0,0)$$

for the long, short, short and long edge respectively: families 0, 1 and 4 are each nonzero on exactly two edges with opposite signs, families 2 and 3 on none, every family sums to zero, and the four vectors sum to the zero vector, as the closed boundary requires. Family 0 is nonzero on edges of two *different* direction classes, $144°$ and $36°$ (likewise families 1 and 4): a family with a nonzero crossing value need not be confined to a single direction class.

The corresponding data for the dart, and the admissible restriction of both, are collected in Table 2.1, so that Lemma 3.15 and Proposition 3.6 can be checked by hand.

class	length	Δ^{raw}	$S(v-u)$	Δ (restricted)	complementary representative
K0	long	$(1,0,0,0,1)$	$\{0,4\}$	$(1,0,0,0,1)$	$(0,-1,-1,-1,0)$
K1	short	$(0,1,0,0,0)$	$\{1\}$	$(0,1,0,0,0)$	$(-1,0,-1,-1,-1)$
K2	short	$(0,0,0,0,-1)$	$\{4\}$	$(0,0,0,0,-1)$	$(1,1,1,1,0)$
K3	long	$(-1,-1,0,0,0)$	$\{0,1\}$	$(-1,-1,0,0,0)$	$(0,0,1,1,1)$
D0	short	$(-1,-1,0,0,0)$	$\{1\}$	$(0,-1,0,0,0)$	$(1,0,1,1,1)$
D1	long	$(1,1,0,0,0)$	$\{0,1\}$	$(1,1,0,0,0)$	$(0,0,-1,-1,-1)$
D2	long	$(-1,0,0,0,-1)$	$\{0,4\}$	$(-1,0,0,0,-1)$	$(0,1,1,1,0)$
D3	short	$(1,0,0,0,1)$	$\{4\}$	$(0,0,0,0,1)$	$(-1,-1,-1,-1,0)$

Table 2.1: Signed crossing vectors of all eight half-edge classes on the reference prototiles of Definition 2.6, computed from the offsets (2.1). Column Δ^{raw} counts every chord of $\mathcal{A}$ meeting the directed side; Δ keeps only the families in the admissible set $S(v-u)$ of Definition 3.1. The last column is the second admissible representative of the edge vector, obtained by subtracting $(1,1,1,1,1)$ up to sign (Remark 2.12). Three features of the table are used later. The restricted vector Δ coincides with the minimal-support representative in all eight rows, which is Lemma 3.15. The raw vector does so in six rows but not at D0 or D3, where it has support 2 while the two admissible representatives have supports 1 and 4, which is Proposition 3.6*(ii)*; the discrepancy is $\Delta^{\mathrm{raw}} - \Delta = \mp\mathbf{n}_0$, the family-0 notch chord. Finally each prototile's four raw vectors sum to zero, as a closed boundary requires.

3. The Crossing Data: Count and Position

This section assembles the detection data. The signed bar-crossing count of an edge is a function of the edge vector alone, so its agreement across a shared edge holds unconditionally (Proposition 3.16): the lower bound of the hierarchy. The organizing statement of the section is Proposition 3.19: agreement of the count *together with the crossing position* is equivalent to the matching rules, edge by edge, on arbitrary candidate tilings. The proposition is a positional relabeling of the classical criterion (Remark 3.20). Its role is to express the rule in the positional coordinates on which the quotient analysis runs. Section 4 then forms the compatibility quotient of the matching rule and shows that the three-chord signature realizes it, which is the paper's main theorem.

3.1. Tile-side crossing data and the gluing conditions

The crossing datum is built in two stages: a *tile-side* (half-edge) function defined from each tile's own decoration alone, and a gluing condition obtained by comparing the two tile-side values on each shared edge. A position-recording enrichment is introduced in Definition 3.7.

Definition 3.1 (Tile-side bar-crossing function)**.** Let $\mathbf{n}_0, \ldots, \mathbf{n}_4$ be the five bar-family unit normals. For each tile $t \in \mathcal{T}$ and each directed edge $(u \to v)$ on the boundary ∂t, define

$$\Delta^{(t)}_{\mathbf{n}_k}(u \to v) := \begin{cases} \operatorname{sign}\big(\mathbf{n}_k \cdot (v-u)\big) & \text{if } k \in S(v-u) \text{ and a family-}k \text{ chord of } t \\ & \text{crosses } \{u,v\}, \\ 0 & \text{otherwise,} \end{cases} \tag{3.1}$$

where $S(v-u) \subseteq \{0,\ldots,4\}$ is the *admissible index set* of the edge vector, namely the support of the unique minimal-support representative of $v-u$ furnished by Lemma 2.11(ii) and Remark 2.12: thus $S = \{k\}$ for a short edge $\pm\mathbf{n}_k$ and $S = \{j, j+1\}$ for a long edge $\pm(\mathbf{n}_j + \mathbf{n}_{j+1})$. Here "local bar chord of t" refers to a connected component of the intersection of a bar line with t, determined solely by t's own Penrose decoration (Definition 2.3), with no reference to adjacent tiles. The case distinction is unambiguous because at most one chord of any *single* family crosses a given edge (Remark 2.5(ii)), so $\Delta^{(t)}_{\mathbf{n}_k}(u \to v) \in \{-1, 0, +1\}$. Reversing the edge reverses the sign while fixing S, so the function is antisymmetric on ∂t.

Remark 3.2 (Why the restriction to $S(v-u)$ is not optional). The decoration does place crossings of inadmissible families on some edges, and two finite computations over the eight half-edge classes, with the offsets (2.1), show that the apparatus of this section fails if they are counted.

(i) The reconstruction identity

$$v - u \;=\; \sum_{k=0}^{4} \Delta_{\mathbf{n}_k}(u \to v)\, \mathbf{n}_k \tag{3.2}$$

holds with the restriction at all eight half-edge classes, hence at every edge of every candidate tiling. Without the restriction it fails at two of the eight, namely at the dart's two short edges, where the dart's family-0 notch chord contributes a second nonzero entry and the sum has length φ instead of 1. Indeed no two-element signed combination of the $\mathbf{n}_k$ is a unit vector, since $|\mathbf{n}_j \pm \mathbf{n}_l| \in \{2\cos 36°, 2\cos 72°, 2\sin 36°, 2\sin 72°\}$ and 1 is not among these. A short edge therefore *cannot* carry two admissible crossings, and an unrestricted formulation has no reconstruction equation.

(ii) With the restriction the crossing vector is edge-determined (Lemma 3.15). Without the restriction that fails at ten of the twenty edge vectors, precisely because a kite short edge and a dart short edge carry different raw crossing sets. The discarded chord is exactly the one *not* continuing across the edge in question: a chord terminating near the dart's reflex vertex.

Two things should be distinguished here. That the support of the count is $S(v-u)$ is a definition. That every admissible family actually crosses, so that the second clause of (3.1) never fails for $k \in S(v-u)$ over legal one-sided placements, is a geometric fact, verified by the finite enumeration of Lemma 3.15.

That enumeration gives the restricted count as the minimal-support representative of the edge vector identically, for every tile, edge, family and placement, which is Lemma 3.15(a). What the restriction discards is exactly the decoration-dependent part of the raw count (Proposition 3.6), so the restricted count is a function of the edge vector alone and carries no information about the decoration: (3.2) holds of it by the displayed identity. The geometric content of the enriched datum resides in the position τ of Definition 3.7.

Definition 3.3 (The two-coloring of the vertices)**.** Color the vertices of each prototile as follows: on the kite the two vertices on the axis of symmetry (the $72°$ apex and the $144°$ vertex) receive one color, its two wings the other. On the dart the assignment is reversed, so that its $216°$ reflex vertex and $72°$ tip receive the wings' color. Write A for the color of the kite's axis vertices. The edge labels of Definition 2.6 are the eight *half-edge classes*.

For the star sequences below, the corner written $\mathsf{X}a$ is the prototile corner at which the directed boundary edge $\mathsf{X}a$ begins, so its incoming edge is $\mathsf{X}(a-1)$ (indices mod 4) and its outgoing edge is $\mathsf{X}a$; superscripts denote repetition.

Lemma 3.4 (The two-color rule yields exactly the classical vertex stars)**.** *Color the prototile vertices as in Definition 3.3, and call a cyclic sequence of prototile corners a* legal star *if consecutive corners meet along edges of equal length whose color pairs are reverses of one another, and the corner angles sum to* $360°$*. Then:*

(i) *There are exactly eight legal unordered pairs of half-edge classes, namely* $\mathsf{D0}|\mathsf{D3}$*,* $\mathsf{D0}|\mathsf{K2}$*,* $\mathsf{D1}|\mathsf{D2}$*,* $\mathsf{D1}|\mathsf{K3}$*,* $\mathsf{D2}|\mathsf{K0}$*,* $\mathsf{D3}|\mathsf{K1}$*,* $\mathsf{K0}|\mathsf{K3}$ *and* $\mathsf{K1}|\mathsf{K2}$*. Of these, seven are realizable,* $\mathsf{D0}|\mathsf{D3}$ *being excluded because it identifies two* $216°$ *reflex vertices, giving* $432° > 360°$*.*

(ii) *Discarding the stars that use the pairing* $\mathsf{D0}|\mathsf{D3}$*, exactly* seven *legal stars remain, namely*

$$\mathsf{K0}^5,\quad \mathsf{D2}^5,\quad \mathsf{D0\,K3\,K1},\quad \mathsf{D1\,D3\,K2\,K2},\quad \mathsf{D1\,K0\,K0\,D3\,K2},$$
$$\mathsf{D2}^3\mathsf{K1\,K3},\quad \mathsf{D2\,K1\,K3\,K1\,K3},$$

which are the sun, star, ace, deuce, jack, king and queen [GS87, §10.3], [BG13, §6.2]; the seven are also drawn, with these names, in the Tilings Encyclopedia [HF].

(iii) *Consequently every valid tiling of the plane contains darts: the only dart-free legal star is the sun, whose corners are five kite* $72°$ *apexes, and every legal star containing a kite corner other than that apex contains a dart. Since every kite has such corners, no valid tiling is dart-free, and darts occur with positive density.*

Proof. All three parts are finite enumerations. For *(i)*, compare the 8 half-edge classes pairwise on length and color pair. The dart's interior angles are $216°$ at the reflex vertex, $72°$ at the tip and $36°$ at each wing, so D0 has endpoint angles $(216°, 36°)$ and D3 has $(36°, 216°)$, and gluing them identifies the reflex vertices, giving $216 + 216 = 432$, and the wings, giving $36 + 36 = 72$. For *(ii)*, enumerate cyclic sequences of corners subject to the two conditions, counted up to cyclic rotation, mirror-image sequences counted separately when distinct. There are 17, of which 10 use the pairing $\mathsf{D0}|\mathsf{D3}$ somewhere and are excluded by *(i)*. The order of the two steps matters: the $432°$ obstruction at a $\mathsf{D0}|\mathsf{D3}$ edge occurs at the *far* endpoint of that edge, not at the vertex being enumerated, so a purely per-vertex enumeration does not detect it and returns all 17. The excluded ten are built from repeated dart wing corners, the largest being $(\mathsf{D1\,D3})^5$, ten darts each presenting a $36°$ wing. For *(iii)*, inspect the seven stars of *(ii)*. □

Remark 3.5 (Status of the vertex-coloring formulation). The two-coloring of Definition 3.3 is the classical vertex-coloring formulation of the P2 matching rule. Grünbaum and Shephard present the rule through vertex markings of exactly this pattern, equivalent to the arrow and arc decorations of the same source [GS87, §10.3]; that equivalence is classical and is used here by citation, not reproved. The eight pairs of Lemma 3.4*(i)* are the marking-legal pairs of the rule in this formulation. The seven-star classification is likewise classical and the citations locate it, but it is re-derived from the coloring in the proof above, because the derivation is three lines and because Lemma 3.4*(i)* is needed in the same form. No step of this paper rests on the reader accepting the list on authority.

Proposition 3.6 (The raw chord count is neither an admissible representative nor a necessary gluing condition)**.** *Let* $\Delta^{\mathrm{raw}}_{\mathbf{n}}(u \to v)$ *denote the signed count of* all *chords of* (2.1) *crossing* $\overline{uv}$*, irrespective of the family index. Then:*

(i) *At six of the eight half-edge classes—both kite long edges, both kite short edges, and both dart long edges—*Δ^{raw} *coincides with the minimal-support representative of the edge vector.*

(ii) *At the dart's two short edges* Δ^{raw} *is not an admissible representative* at all*: it has support* 2*, whereas the two admissible representatives there have supports* 1 *and* 4*, and*

$$\sum_{k=0}^{4} \Delta^{\mathrm{raw}}_{\mathbf{n}_k}(u \to v)\, \mathbf{n}_k - (v-u) \;=\; \mp\,\mathbf{n}_0,$$

the defect being exactly the family-0 *notch chord. In particular* (3.2) *fails there.*

(iii) Δ^{raw}*-agreement is not even a* necessary *condition for validity. In any valid tiling the only realizable legal partner of a dart short edge is a kite short edge, and across such an edge the dart contributes two chords and the kite one, so* Δ^{raw} *disagrees. Hence* Δ^{raw}*-gluing fails at* every *interior dart short edge of* every *valid tiling.*

Proof. *(i)* and *(ii)* are read off the raw crossing sets (2.2): an inadmissible family contributes only at the dart short edges, where family $\mathbf{n}_0$ contributes and the perpendicular families are $\mathbf{n}_1, \mathbf{n}_4$ (Remark 2.9). Inadmissibility is the metric fact of Remark 3.2*(i)*, and the supports 1 and 4 of the admissible representatives are computed in Remark 2.12. For *(iii)*, by Lemma 3.4*(i)* the only realizable legal partner of a dart short edge is a kite short edge, across which the kite contributes one chord and the dart two by (2.2). Every valid tiling contains darts (Lemma 3.4*(iii)*), and every edge is interior. □

Definition 3.7 (Enriched tile-side crossing datum)**.** Let t be a tile, $\mathbf{n}_k$ a bar-family normal and $(u \to v)$ a directed edge of ∂t. If $k \in S(v-u)$ *and* a local bar chord of family $\mathbf{n}_k$ of the assignment $\mathcal{A}$ in t crosses the edge $\{u, v\}$, let

$$\tau^{(t)}_{\mathbf{n}_k}(u \to v) \;\in\; (0,1)$$

be the position of the crossing point along the edge, normalized so that u is at 0 and v is at 1. Otherwise set $\tau^{(t)}_{\mathbf{n}_k}(u \to v) := \varnothing$. The restriction to $k \in S(v-u)$ is the one imposed on Δ in

Definition 3.1, and falls on the same chord: on the dart's two short edges it discards the position of the family-0 notch crossing, exactly as Δ discards its sign (Remark 3.2, Proposition 3.6). The *enriched tile-side crossing datum* is the pair

$$\widehat{\Delta}^{(t)}_{\mathbf{n}}(u \to v) := \big(\Delta^{(t)}_{\mathbf{n}}(u \to v),\ \tau^{(t)}_{\mathbf{n}}(u \to v)\big). \tag{3.3}$$

It is well defined by Remark 2.5(i) (no bar passes through a vertex, so $\tau \neq 0, 1$) and (ii) (at most one chord of a given family crosses a given edge, so τ is a single value). Reversing the edge acts by $\Delta \mapsto -\Delta$ and $\tau \mapsto 1-\tau$, so $\widehat{\Delta}$ is antisymmetric in the sense that $\widehat{\Delta}^{(t)}_{\mathbf{n}}(v \to u) = (-\Delta^{(t)}_{\mathbf{n}}(u \to v), 1-\tau^{(t)}_{\mathbf{n}}(u \to v))$. Like $\Delta^{(t)}_{\mathbf{n}}$, it is determined by t's own decoration alone (Definition 2.3).

Definition 3.8 (Enriched gluing condition)**.** A candidate tiling satisfies the *enriched gluing condition* at an interior edge $\{u, v\}$ shared by tiles A and B if

$$\widehat{\Delta}^{(A)}_{\mathbf{n}_k}(u \to v) = \widehat{\Delta}^{(B)}_{\mathbf{n}_k}(u \to v) \qquad \text{for all } k \in S(v-u). \tag{3.4}$$

Quantifying over $k \in S(v-u)$ rather than over all five families is not a weakening: outside $S(v-u)$ both components are $\varnothing$ or 0 by Definition 3.7, so those families would contribute nothing to the comparison in any case.

Lemma 3.9 (Edge-local dictionary)**.** *Color the vertices of each prototile as in Definition 3.3. Then, for both prototiles simultaneously and for every placement:*

(i) On a short edge the unique admissible crossing lies at distance $\frac{1}{4}$ from the endpoint colored A. On a long edge the two admissible crossings coincide at a single point, at distance $\frac{1}{2\varphi} = \frac{\sqrt{5}-1}{4}$ from the endpoint colored A. Equivalently, in the normalized parameter τ of Definition 3.7,

$$\tau \in \{\tfrac{1}{4}, \tfrac{3}{4}\} \text{ on a short edge}, \qquad \tau \in \Big\{\tfrac{3-\sqrt{5}}{4}, \tfrac{1+\sqrt{5}}{4}\Big\} \text{ on a long edge}, \tag{3.5}$$

the two values in each class being exchanged by $\tau \mapsto 1-\tau$, and each determining the coloring of the two endpoints. Throughout the paper the two long-edge values are abbreviated $\beta = \frac{3-\sqrt{5}}{4}$ and $\gamma = \frac{1+\sqrt{5}}{4} = 1-\beta$.

(ii) Consequently the map from the marking one side places on the edge to the admissible enriched datum that side contributes is injective on each edge class, and its inverse is the reading in (i).

(iii) Consequently, at every interior edge of every candidate tiling, the enriched gluing condition (3.4) holds if and only if *the matching rule holds at that edge. Of the sixteen marking-legal ordered pairs of half-edge classes, fourteen are realizable in valid tilings,* D0|D3 *and its reverse being excluded by the $432°$ obstruction of Lemma 3.4(i).*

Proof. All three parts are finite verifications over the eight half-edge classes Ka, Da of Definition 3.3.

(i). The admissible crossings computed from (2.1) are, with the counterclockwise color pair of each class alongside,

$$\begin{array}{llll} \mathsf{K0},\ \mathsf{D1} & \text{long} & (A,B) & \tau=\frac{3-\sqrt{5}}{4}, \\ \mathsf{K3},\ \mathsf{D2} & \text{long} & (B,A) & \tau=\frac{1+\sqrt{5}}{4}, \\ \mathsf{K2},\ \mathsf{D3} & \text{short} & (A,B) & \tau=\frac{1}{4}, \\ \mathsf{K1},\ \mathsf{D0} & \text{short} & (B,A) & \tau=\frac{3}{4}, \end{array}$$

which is (3.5). In each row the distance from the A-colored endpoint is $\frac{1}{4}\cdot 1=\frac{1}{4}$ or $\frac{3-\sqrt{5}}{4}\cdot\varphi=\frac{\sqrt{5}-1}{4}$ as claimed. The value of τ depends only on the edge length and the coloring, not on the prototile. On a long edge the two crossing families meet the edge at the *same* point, so the long-edge datum is a single position and not a pair. For the kite that coincidence is structural, its three offsets being equal and its $72°$ apex equidistant from the three bars. For the dart, whose family-0 offset $\frac{2-\sqrt{5}}{4}$ differs from its family-1 and family-4 offsets $-\frac{3}{4}$, it is a coincidence of (2.1), verified but not ascribable to a symmetry.

(ii). The two admissible markings on an edge of given length yield the values τ and $1-\tau$, distinct because $\tau\neq\frac{1}{2}$ in both classes. Δ contributes nothing further, being a function of the edge alone (Lemma 3.15).

(iii). Place both incident tiles against a common directed edge and read τ from a common endpoint: enriched gluing says the two contributed data coincide, which by (ii) says the two markings coincide, which is the matching rule at that edge. Direct verification over all 32 ordered pairs of half-edge classes of equal length confirms this: enriched gluing holds at exactly the 16 marking-legal pairs and fails at the other 16, with no exceptions. That verification is displayed as Table 3.1. It is a one-line criterion: the second tile traverses the shared edge oppositely, so it contributes $1-\tau$ where its own class contributes τ, and (3.4) therefore holds at the ordered pair $s|s'$ precisely when $\tau(s)+\tau(s')=1$. With the four values of (3.5) this is decidable by inspection, since $\frac{1}{4}+\frac{3}{4}=1$ and $\beta+\gamma=1$ are the only coincidences available. For the realizability count, "realizable" means occurring at an interior edge of some valid tiling of the plane, as Definition C.1 requires. The pair $\mathsf{D0}|\mathsf{D3}$ and its reverse are excluded by the $432°$ obstruction of Lemma 3.4*(i)*. Each of the seven remaining unordered pairs occurs among the consecutive-corner pairings of the seven legal stars of Lemma 3.4*(ii)*: the ace realizes $\mathsf{D0}|\mathsf{K2}$, $\mathsf{D3}|\mathsf{K1}$ and $\mathsf{K0}|\mathsf{K3}$, the deuce adds $\mathsf{K1}|\mathsf{K2}$ and $\mathsf{D1}|\mathsf{D2}$, and the king adds $\mathsf{D2}|\mathsf{K0}$ and $\mathsf{D1}|\mathsf{K3}$. Every one of the seven stars occurs in every Penrose kite–dart tiling of the plane: the seven are the complete list of vertex neighborhoods of the P2 tilings, each occurring with positive frequency [GS87, §10.5], [BG13, §6.2]. Hence all fourteen ordered pairs are realizable. The certified patch exhibits all seven unordered pairs among its 670 interior gluings (Remark 4.9). □

short edges					long edges				
	s'					s'			
s	K1	K2	D0	D3	s	K0	K3	D1	D2
$\tau(s)$	$\frac{3}{4}$	$\frac{1}{4}$	$\frac{3}{4}$	$\frac{1}{4}$	$\tau(s)$	β	γ	β	γ
K1	–	✓	–	✓	K0	–	✓	–	✓
K2	✓	–	✓	–	K3	✓	–	✓	–
D0	–	✓	–	(✓)	D1	–	✓	–	✓
D3	✓	–	(✓)	–	D2	✓	–	✓	–

Table 3.1: The enriched gluing condition (3.4) on all 32 ordered pairs $s|s'$ of half-edge classes of equal length, the verification behind Lemma 3.9(iii). Cross-length pairs are omitted because they cannot share an edge. A mark records that gluing holds, equivalently that $\tau(s) + \tau(s') = 1$ for the values of (3.5) listed in the third row; a dash records that it fails. Gluing holds at 8 of the 16 short pairs and 8 of the 16 long pairs, so at exactly 16 of the 32, and these are precisely the marking-legal pairs. The two parenthesized entries are D0|D3 and its reverse: marking-legal, and excluded from the partner sets of §4 by the $432°$ obstruction of Lemma 3.4*(i)* rather than by the local criterion. Discarding them leaves the 14 realizable ordered pairs, that is the 7 unordered pairs listed in the proof above.

3.2. The chord offsets are forced within the ansatz

Proposition 3.10 (The notch chord is forced within the three-chord ansatz)**.** *Suppose each prototile carries one chord line in each of three bar families, the kite's three lines being those of* (2.1)*, and suppose the chords are required to continue collinearly—the two chord segments on the two sides of a shared edge lie on one line, in particular in the same bar family, meeting the edge at the same point—across every legal edge of a valid tiling. Then the dart's three families are* $\{0, 1, 4\}$*, and the dart's three lines are those of* (2.1)*: its family-*1 *and family-*4 *offsets are* $-\frac{3}{4}$*, and its family-*0 *offset is uniquely* $\frac{2-\sqrt{5}}{4}$*, a value lying strictly between the dart's reflex vertex and its wings, so the family-*0 *line necessarily cuts both of the dart's short edges. The notch chord of* (2.1) *is therefore forced, not chosen.*

Proof. Only the kite-side crossing values are used as input, so that nothing derived here about the dart is presupposed: the kite entries below are computed from the kite offsets of (2.1) alone, as in the kite rows of Appendix A. The three families are determined first. Across the short-edge gluings the dart's partners contribute their perpendicular chords, which lie in the families perpendicular to those edges, namely 1 and 4; across the long-edge gluings the kite's two admissible crossings coincide, and collinear continuation forces the dart to carry a chord of the remaining family 0 through that point. Hence the dart's three families are $\{0, 1, 4\}$, and it remains to determine the three offsets. The dart's family-1 offset is determined first. Across the short-edge gluing D0|K2 the kite's chord meets the edge at $\frac{3}{4}$ from the identified reflex vertex (kite rows of Lemma 3.9(i)), and $\mathbf{n}_1 \cdot (Z' - X) = -1$ on the dart's edge D0, so collinear continuation forces the dart's family-1 offset to $-\frac{3}{4}$; the mirror gluing D3|K1 forces the family-4 offset to $-\frac{3}{4}$. The kite's two admissible crossings on a long edge coincide (kite rows of Lemma 3.9(i)). A dart long edge's legal partner is a kite long edge (Lemma 3.4), so collinear continuation forces the dart's two admissible long-edge crossings to coincide too. On D1 ($Z' \to Y$) the family-1 chord meets the edge at $\tau = \frac{3-\sqrt{5}}{4}$. Requiring the family-0 crossing there is one linear equation, $c_0 = -\cos 72° + \frac{3-\sqrt{5}}{4}(1+\cos 72°) = \frac{2-\sqrt{5}}{4}$, so c_0 is unique. The dart's $\mathbf{n}_0$-coordinates are 0 at the reflex vertex and $-\cos 72°$ at the wings, and $\frac{2-\sqrt{5}}{4}$ lies strictly between, so the family-0 line cuts both short edges (Remark 2.8). □

Remark 3.11 (What Proposition 3.10 does not establish). The hypotheses of Proposition 3.10 are two, and neither is proved anywhere in this paper. The first is the three-chord *ansatz*: that each prototile carries one chord line in each of exactly three bar families. The second is the kite's three offsets $\frac{1}{4}$ of (2.1).

Both are read off the classical decoration, as Remark 2.7 records, and are taken here as the definition of $\mathcal{A}$. What the proposition establishes is conditional: *given* those two inputs, the dart's three families and all three of its offsets are forced by collinear continuation, with no further freedom. Why three families rather than two or four, and why $\frac{1}{4}$ rather than another value, are not answered. We are not aware of a published derivation of either from a minimality or uniqueness principle, and supplying one would strengthen the proposition; it would not affect Theorem 4.3, which is a statement about $\mathcal{A}$ as defined by (2.1) and does not depend on $\mathcal{A}$ being the only possible choice.

One half of the ansatz admits a direct derivation from the quotient itself. A two-family assignment on the kite places at most two chords on any edge, so its per-edge signature takes at most the values of those two chords; but the quotient has six classes by Proposition 4.1, and a realizing signature must take six distinct values. Three families is therefore the *minimum* compatible with realizing the quotient, not merely the count read off the classical figure. The kite offset $\frac{1}{4}$ remains the genuinely classical input: deriving it would require a minimality principle on the offset itself, and we do not claim one.

3.3. The signed count carries no information

Definition 3.12 (The count gluing condition)**.** Fix a family $\mathbf{n}$ and call

$$\Delta_{\mathbf{n}}^{(A)}(u \to v) = \Delta_{\mathbf{n}}^{(B)}(u \to v) \tag{3.6}$$

the *count* gluing condition at an interior edge $\{u, v\}$ shared by tiles A and B.

Remark 3.13 (The restriction in the comparison is not cosmetic, and the comparison is patch-local). Agreement of the $\varnothing$-values does *not* say that no chord terminates on the edge, since families outside $S(v-u)$ are never compared and may terminate there with both sides recording nothing. This occurs on the internal edges of the kite-plus-dart rhombus (Proposition 3.17): there $S = \{1\}$, the family-1 data agree, and the dart's family-0 notch chord terminates unremarked (Remark 2.9).

Because the criterion of Lemma 3.9(iii) compares only the two tiles at a single edge, it applies verbatim to a finite patch, no property of the tiling as a whole entering the comparison. This is what supports the claim in §1.3(ii) that the criterion is available on finite patches.

Remark 3.14 (Status of the classical Ammann-bar biconditional). The forward direction of the classical biconditional—a legal Penrose tiling has continuous bars—is the one used in the classical forcing arguments [GS87, §10.6]. The converse, for an *arbitrary* candidate dart–kite tiling, we have not located in this generality, and the octagonal case shows nothing here is automatic: Socolar's octagonal tiling requires *secondary* Ammann lines, a second decoration beyond the classical one, precisely because the primary lines alone do not force the rules [Soc89]. Nothing below uses the biconditional in either direction: Lemma 3.9 concerns the enriched datum computed from the three chords (2.1), which do not form complete lines (Remark 2.9).

Lemma 3.15 (The crossing vector is edge-determined and represents the edge)**.** *Write* $c(e) := \big(\Delta_{\mathbf{n}_0}, \ldots, \Delta_{\mathbf{n}_4}\big) \in \{-1, 0, +1\}^5$ *for the vector of tile-side values of Definition 3.1 at a directed edge with edge vector* e*. Then:*

(a) $c(e)$ *depends only on* e*. Explicitly, for every* $e \in \mathcal{E}$ *(Lemma 2.10), every side of* e*, and every legally decorated prototile placed with one of its edges on* e *on that side, the resulting* $c(e)$ *is the same, and equals the minimal-support representative of* e*.*

(b) Consequently $\sum_k c_k(e)\, \mathbf{n}_k = e$*, i.e.* (3.2) *holds at every edge of every candidate tiling.*

Proof. By Lemma 2.10 the edge vectors are $\{\pm\mathbf{n}_k\} \cup \{\pm(\mathbf{n}_j + \mathbf{n}_{j+1})\}$, twenty directed, ten unordered $\{v, -v\}$ pairs, and a prototile can be laid against each in one of $2 \times 4 = 8$ ways (prototile, which of its four edges; reflected placements coincide with unreflected ones, each decorated prototile being invariant under its own axial reflection, Remark 2.2), of which those matching the edge length survive. Enumerating these and computing the crossing data from (2.1) gives in every case the crossing set $S(e)$ of Definition 3.1 with signs $\operatorname{sign}(\mathbf{n}_k \cdot e)$, the minimal-support representative. This is (a), and (b) follows since that representative represents e by definition. It is the restriction to $S(e)$ that makes (a) true: the *raw* crossing sets differ between kite and dart placements at ten of the twenty directed edge vectors (Remark 3.2). □

Proposition 3.16 (The count gluing condition is vacuous on candidate tilings)**.** *The signed count does not detect the matching rule. Three statements record this, of which the third is the general one and the first two are explicit witnesses of increasing size.*

(i) ***(Unconditional; a two-tile patch.)*** *Some decorated patch of two prototiles meeting along a shared edge satisfies* (3.6) *for all five families while the Penrose matching rule fails at that edge.*
Hence (3.6) *does not imply the matching rule.*

(ii) ***(Unconditional; a tiling of the plane.)*** *There is a* periodic *candidate decorated Penrose tiling of the whole plane at which* (3.6) *holds for all five families at every interior edge, while the matching rule fails at a set of edges of positive density—asymptotically half of them, strictly more than half in every finite block (Proposition 3.17).*

(iii) ***(Unconditional; every candidate tiling.)*** *On every candidate decorated Penrose tiling, valid or not,* (3.6) *holds at every interior edge: the count gluing condition carries no information about matching whatsoever.*

Part (iii) supplies the count-agreement half of both (i) and (ii). What each witness adds is a configuration at which matching demonstrably fails, and that does not follow from (iii).

Proof. (i). Let R be the reflection in the perpendicular bisector of an interior edge $\{u, v\}$ with incident tiles A, B. Then $R(B)$ is a legal placement of the same decorated prototile on the far side of $\{u, v\}$, by the reflection invariance of the decorated prototiles (Remark 2.2), and it presents the reversed marking there, so the two-tile patch $(R(B), B)$ violates the matching rule at $\{u, v\}$. Its count data nevertheless agree, because R carries bar lines to bar lines, the induced permutation ς of the five families preserves the crossing set at the reflected edge, and the sign factor is edge-determined. Remark 3.18 carries out the verification of ς over the ten edge directions and draws the contrast with the enriched datum. Since ς-invariance holds for *both* admissible representatives of every edge vector, the construction is insensitive to the bar convention of Remark 2.9.

(ii) is Proposition 3.17 below.

(iii). Fix a directed edge $(u \to v)$ with incident tiles A, B. By Lemma 3.15(a) the whole crossing vector at $(u \to v)$ is a function of $v - u$ alone, the same for every legal one-sided placement. In particular $\Delta^{(A)}_{\mathbf{n}_k}(u \to v) = \Delta^{(B)}_{\mathbf{n}_k}(u \to v)$ for every k, which is (3.6). □

Proposition 3.17 (The kite-plus-dart rhombus: a periodic sharpness witness)**.** *Place a dart so that its* $216°$ *reflex vertex coincides with a kite's* $144°$ *vertex and its two short edges lie along the kite's two short edges. Concretely, with the reference prototiles of* (2.1)*, translate the dart by* φ *along the kite's axis. The two short edges are consumed,* $144° + 216° = 360°$*, and the union is a rhombus with all four sides of length* φ *and angles* $72°, 108°$*. Let* $\mathcal{R}$ *be the tiling of the plane by the translates of this rhombus under the lattice* $\mathbb{Z}(1+\zeta) + \mathbb{Z}(1+\zeta^4)$*, each subdivided into its kite and dart. Then* $\mathcal{R}$ *is an edge-to-edge candidate decorated Penrose tiling in the sense of Definition 2.1, the count gluing condition* (3.6) *holds for all five families at every interior edge of* $\mathcal{R}$*, and the matching rule fails at exactly the two kite/dart interfaces interior to each rhombus (Figure 3.1)—a proportion* $162/306$ *of the interior edges of a* 9×9 *block (each of the* 81 *rhombi contributes* 2 *failing interfaces, and the interior edges are these* 162 *together with the* $2 \cdot 9 \cdot 8 = 144$ *sides shared between neighboring rhombi), and asymptotically* $\frac{1}{2}$*.*

The general count is exact. An $N \times N$ *block of rhombi has* $2N^2$ *failing interfaces, two per rhombus, and* $2N(N-1)$ *interior sides shared between neighbors,* $N(N-1)$ *in each of the two lattice directions, hence* $4N^2 - 2N$ *interior edges in all, so the failure proportion is*

$$\frac{2N^2}{4N^2 - 2N} = \frac{N}{2N-1} \xrightarrow[N\to\infty]{} \tfrac{1}{2}, \tag{3.7}$$

which at $N = 9$ *is* $\frac{9}{17} = \frac{162}{306}$*. The proportion exceeds* $\frac{1}{2}$ *at every finite* N *and decreases to it, the excess being the boundary effect of the* $2N$ *sides that a larger block would supply.*

Proof. With $X_{\text{kite}} = 0$ the dart translated by φ has its wings at $1+\zeta$ and $1+\zeta^4$, exactly the kite's wings, and its reflex vertex at φ, the kite's $144°$ vertex. The quadrilateral $0,\ 1+\zeta^4,\ \varphi^2,\ 1+\zeta$ has all four side vectors of modulus $|1+\zeta| = 2\cos 36° = \varphi$, and $(1+\zeta)+(1+\zeta^4) = 2+2\cos 72° = \varphi^2$ confirms it is the parallelogram spanned by the two edge vectors. Hence the lattice of those vectors tiles the plane by the rhombus, and $\mathcal{R}$ is edge-to-edge with every interior edge carrying exactly two tiles. Its edge vectors are $\pm\mathbf{n}_k$ and $\pm(\mathbf{n}_j + \mathbf{n}_{j+1})$, so it satisfies Lemma 2.10 and is a candidate tiling.

Count gluing holds by Proposition 3.16(iii), and directly at the offending edges, which are exactly those where the raw chord counts differ: on an interior kite-short/dart-short edge the kite is met by one chord and the dart by two (Remark 2.9), the dart's extra chord being its family-0 notch chord, inadmissible for a short edge and hence uncounted, so both sides contribute the same value $\operatorname{sign}(\mathbf{n}_k \cdot (v-u))$ in the perpendicular family and 0 in the other four.

Matching fails at those edges: in the notation of Definition 3.3 the half-edge classes meeting there are K1|D0 and K2|D3, neither of them one of the seven legal pairs, since the legal short-edge pairs are K1|K2, K1|D3 and K2|D0. Equivalently, and this is the classical statement, the arrows on the two short edges disagree.

The rhombus boundary edges K0|D2 and K3|D1 are legal, so the failure density is $\frac{1}{2}$ rather than 1. □

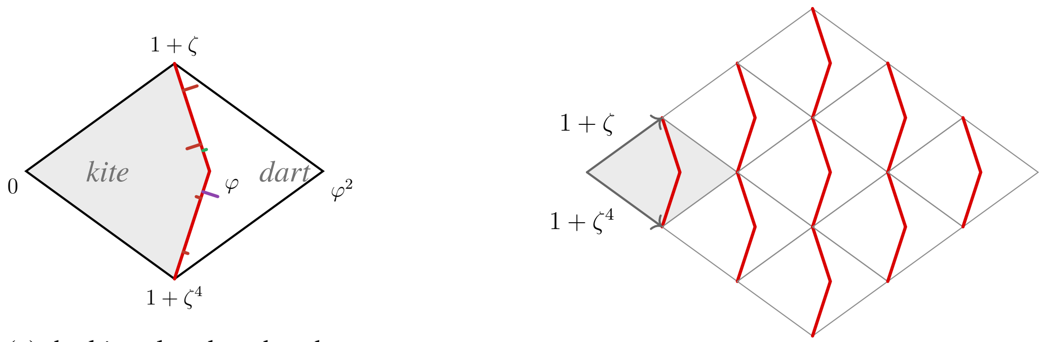

(a) the kite-plus-dart rhombus

(b) the periodic tiling $\mathcal{R}$

Figure 3.1: The periodic sharpness witness of Proposition 3.17. (a) The kite-plus-dart rhombus $0,\ 1+\zeta^4,\ \varphi^2,\ 1+\zeta$ of side φ: the dart, translated by φ along the kite's axis, consumes the kite's two short edges. One-sided stubs show the chords each tile brings to a shared short edge: the kite brings its single perpendicular chord. The dart brings a perpendicular chord and its notch chord (relative families 3 and 2), inadmissible on a short edge and invisible to the signed count. The count gluing condition therefore holds at the interface while the matching rule fails there (red edges, the illegal pairs K1|D0 and K2|D3). The four boundary edges meet legally. (b) The lattice tiling $\mathcal{R}$ under $\mathbb{Z}(1+\zeta)+\mathbb{Z}(1+\zeta^4)$: count gluing holds at every edge, and the matching rule fails at the red interfaces—asymptotically half of all interior edges. In both panels red marks failing edges, black legal ones, and grey fill distinguishes kite from dart.

Remark 3.18 (The signed count cannot detect the matching rules). Consider the two-tile patch $(R(B), B)$ of the proof of Proposition 3.16(i), sharing the edge $\{u, v\}$ with the matching rule failing there, R being the reflection in the perpendicular bisector of $\{u, v\}$. Carrying bar lines to bar lines, R permutes the five families by $\varsigma\colon \alpha \mapsto 2\theta - \alpha \pmod{180^\circ}$, where θ is the direction of $\{u, v\}$, and a direct check over the ten edge directions shows ς preserves the crossing set: on a short edge $\pm\mathbf{n}_k$ it fixes k and pairs up the remaining four families. On a long edge $\pm(\mathbf{n}_j + \mathbf{n}_{j+1})$ it exchanges $j \leftrightarrow j+1$ and $j-1 \leftrightarrow j+2$ while fixing $j+3$. The two admissible representatives at each edge being a set and its complement (Remark 2.12), ς-invariance holds for either, and the sign factor is edge-determined, so $\Delta_{\mathbf{n}}^{(R(B))}(u \to v) = \Delta_{\mathbf{n}}^{(B)}(u \to v)$ for all five families while the matching rule fails at $\{u, v\}$, which is the construction used in the proof of Proposition 3.16(i).

The enriched datum detects the reflected placement at the very edge where the marking is reversed. Since R acts on positions by $\tau \mapsto 1 - \tau$ and on families by ς, detection requires $\tau_{\mathbf{n}_i} \neq 1 - \tau_{\mathbf{n}_{\varsigma(i)}}$ for some i. By Lemma 3.9(i) the positions take only the four values (3.5), and the two discriminants are

$$\tau_{\mathbf{n}_k} - \tfrac{1}{2} = \pm\tfrac{1}{4} \quad \text{(short edge)}, \qquad \tau_{\mathbf{n}_j} + \tau_{\mathbf{n}_{j+1}} - 1 = \pm\varphi^{-1} \quad \text{(long edge)},$$

the long-edge crossings coinciding, neither vanishing. The negative statement (i) does not use (3.5) at all, needing only the Δ-invariance above. The matching rules constrain *where* a bar meets an edge, and a $\{-1, 0, +1\}$-valued count records only *whether* one does. Classical Ammann-bar forcing works because bars must continue *straight*, and straightness is a statement about position.

3.4. The position-carrying datum detects the rule

Proposition 3.19 (Enriched gluing is the matching rule)**.** *Let $\mathcal{T}$ be a candidate decorated Penrose tiling in the sense of Definition 2.1 (not necessarily satisfying the matching rules). The following conditions are equivalent:*

(i) ***(Matching rules.)*** *$\mathcal{T}$ satisfies the Penrose matching rules (edge decorations are consistent across all shared edges).*

(ii) ***(Enriched gluing.)*** *The enriched gluing condition (3.4) holds on every interior edge of $\mathcal{T}$, where the crossing data are computed from the three-chord assignment $\mathcal{A}$ of (2.1) and restricted to the minimal support $S(v - u)$ of the edge vector (Definition 3.1).*

Both implications are edge by edge, by the finite dictionary of Lemma 3.9.

There is deliberately no bar-continuity clause: for the three-chord assignment $\mathcal{A}$ such a clause is false on every valid tiling, because of the dart-notch gap (Remark 2.9).

Remark 3.20 (The equivalence is a change of coordinates). On a directed edge Δ carries no information (Lemma 3.15) and τ exactly one bit—which endpoint is colored A—so the equivalence is a relabeling of the classical criterion, not a new local rule. Its content is that Lemma 3.9, an eight-entry table, makes the criterion edge-local and provable on finite patches. Section 4 determines what the same chord data detect beyond the single edge: the whole partner set, exactly.

Proof. (i) $\Rightarrow$ (ii). The two tiles place the same marking at $\{u, v\}$, and each tile's contributed datum is a function of the marking it places (Lemma 3.9(i)), so the data agree. Both Δ and τ are restricted to the admissible families (Definitions 3.1 and 3.7). Without that restriction on τ the implication fails at every ace.

(ii) $\Rightarrow$ (i). By Lemma 3.9(iii), agreement of the enriched data at an edge forces the two markings there to agree. $\square$

4. The Compatibility Quotient and the Three-Chord Signature

Proposition 3.19 characterizes validity edge by edge: the enriched data agree across an edge if and only if the markings do. We now turn to the companion question *inside* the rule. The color of a half-edge does not determine its partner set: several classes may present the same colored edge across a gluing yet differ in which partners they accept. We prove that the three-chord assignment $\mathcal{A}$ of (2.1) already detects the whole partner set, exactly, and that it is the coarsest datum with this property. Formally this is the Myhill–Nerode quotient of the matching rule, computed and realized by the bar geometry.

For P2 the computation is a finite enumeration over the eight half-edge classes.

For the P2 rule the objects are concrete. Let $\Sigma = \{\mathsf{K}a, \mathsf{D}a : a = 0, 1, 2, 3\}$ be the set of the eight half-edge classes of Lemma 3.4. For $s, s' \in \Sigma$ write $s|s'$ when (s, s') is one of the fourteen realizable legal ordered pairs of Lemma 3.9. The *partner set* of s is $P(s) = \{s' \in \Sigma : s|s'\}$, two classes are *compatible-equivalent*, $s \sim s'$, when $P(s) = P(s')$, and $\Sigma/\!\sim$ is the *compatibility quotient* of the P2 rule. The same partition, for an arbitrary finite-range edge-matching rule, is the Myhill–Nerode equivalence [Myh57, Ner58, HU79] of the rule; the general definition, together with the notions of a *signature* and of a signature *realizing* the quotient, is recorded in Appendix C (Definition C.1).

Proposition 4.1 (The quotient has six classes)**.** *$\Sigma/\!\sim$ has exactly six classes, listed in Table 4.1 together with their partner sets. In particular the compatibility relation is strictly finer than the four-class coloring relation of Lemma 3.9: the two short color classes each split in two.*

Proof. Immediate from the pair list of Lemma 3.4*(i)*: the seven realizable unordered pairs give the partner sets of Table 4.1, and the six rows of that table are pairwise distinct. The coloring relation has the four classes (short,AB), (short,BA), (long,AB), (long,BA). The rows $\{\mathsf{D}0\}$, $\{\mathsf{K}1\}$ refine (short,BA) and $\{\mathsf{D}3\}$, $\{\mathsf{K}2\}$ refine (short,AB), while the two long rows are the long color classes. □

Table 4.1: The six-class compatibility quotient of the P2 matching rule. Partners from Lemma 3.4*(i)*; edge descriptions refer to the reference prototiles of Definition 2.6; $\beta = \frac{3-\sqrt{5}}{4}$, $\gamma = \frac{1+\sqrt{5}}{4}$.

class	states	partners	edge, length, colors	three-chord signature
$\mathcal{C}_1$	D0	K2	reflex→wing, short, (B, A)	$(0, \frac{3}{4})$, $(3, \beta)$
$\mathcal{C}_2$	D3	K1	wing→reflex, short, (A, B)	$(0, \frac{1}{4})$, $(2, \gamma)$
$\mathcal{C}_3$	K1	D3, K2	wing→ $144°$, short, (B, A)	$(0, \frac{3}{4})$
$\mathcal{C}_4$	K2	D0, K1	$144°$ →wing, short, (A, B)	$(0, \frac{1}{4})$
$\mathcal{C}_5$	D1, K0	D2, K3	wing→tip / apex→wing, long, (A, B)	$(1, \beta)$, $(4, \beta)$
$\mathcal{C}_6$	D2, K3	D1, K0	tip→wing / wing→apex, long, (B, A)	$(1, \gamma)$, $(4, \gamma)$

Definition 4.2 (Three-chord signature of a half-edge class)**.** Let h be a half-edge of class s in a decorated tiling, with directed edge vector of direction index j (the vector being ω^j or $\varphi\,\omega^j$,

$\omega = e^{i\pi/5}$). Each drawn chord of the three-chord assignment $\mathcal{A}$ (2.1) that meets h contributes a pair (r, τ), defined as follows. The *relative family* is $r \equiv 2i - j \pmod 5$, where i is the chord's bar family (normal $\mathbf{n}_i = \omega^{2i}$). The *normalized crossing position* $\tau \in (0, 1)$ is the position of the chord's crossing point along the directed edge, normalized so the initial vertex is at 0 and the terminal vertex at 1. The index r is invariant under rotation of the placement, and changes sign under reflection, exchanging each class with its mirror class. The position is recorded for *every* drawn chord of $\mathcal{A}$ meeting the half-edge, explicitly *without* the admissibility restriction of Definition 3.7: in particular the dart's family-0 notch chord, inadmissible for the count on a short edge, contributes its pair here. The *three-chord signature* $\sigma(s)$ is this set of pairs. It is constant on each class, the assignment $\mathcal{A}$ being fixed per prototile.

The name is deliberately not "Ammann signature". Everything proved below is a statement about σ as just defined, hence about the explicit assignment $\mathcal{A}$ of (2.1); that $\mathcal{A}$ was read off the classical decoration, and in what sense the two agree, is the empirical statement of Remark 2.7, not a theorem. Naming the signature after $\mathcal{A}$ keeps that distinction visible in every statement that uses it.

Theorem 4.3 (The three-chord signature realizes the compatibility quotient)**.** *For all $s, s' \in \Sigma$,*

$$\sigma(s) = \sigma(s') \iff s \sim s'.$$

The six signatures are those of Table 4.1, drawn in Figure 4.1(b): the crossing positions take only the four values $\frac{1}{4}, \frac{3}{4}, \beta, \gamma$ of (3.5), and the six rows are pairwise distinct.

Remark 4.4 (The grade of the proof). The proof of Theorem 4.3 is symbolic and the statement exact. The signature σ is evaluated from the offsets (2.1) by arithmetic in $\mathbb{Q}(\sqrt{5})$, printed in full in Appendix A, so no floating-point quantity enters the theorem or its proof, and in particular no tolerance of the certification pipeline of Appendix B does. The patch computation of Remark 4.9 corroborates the table independently and is not a step in establishing it.

Proof. Evaluate (2.1) on the reference prototiles: a finite computation in $\mathbb{Q}(\sqrt{5})$, eight classes times three chords, carried out in Appendix A, gives the table. Two remarks organize it. On a long edge the two chords meet the edge at the *same* point (Lemma 3.9(i)), so the long signature is a doubled pair. Since that point and the two families depend only on the length and the color pair, D1 and K0 (likewise D2 and K3) have identical signatures, proving $\Leftarrow$ on the long classes. On a short edge the perpendicular chord contributes $(0, \frac{1}{4})$ or $(0, \frac{3}{4})$ by color, and the dart alone carries the second, notch chord (Remark 2.9): at relative family 3 on D0, at relative family 2 on D3. That chord is what separates the dart's short classes from the kite's: without it the rows $\mathcal{C}_1, \mathcal{C}_3$ (and $\mathcal{C}_2, \mathcal{C}_4$) would coincide. All six rows being distinct proves $\Rightarrow$. That two classes in one row share it proves $\Leftarrow$. $\square$

Example 4.5 (One gluing, read from both sides)**.** Consider the realizable pair D3|K1, the short-edge gluing of Remark 2.9. The dart reads its edge $Z \to X$: the perpendicular family-4 chord at $\tau = \frac{1}{4}$ and the notch chord at relative family 2, $\tau = \gamma$. That is the row $\sigma(\text{D3}) = \{(0, \frac{1}{4}), (2, \gamma)\}$. The kite reads the same physical crossings from the other side: traversed oppositely, τ becomes $1 - \tau$ while the relative family is unchanged, so its family-1 chord at $\frac{3}{4}$ mirrors the dart's $(0, \frac{1}{4})$, and the continuation of the notch line registers at $(2, \beta)$, mirroring $(2, \gamma)$ since $1 - \gamma = \beta$. The drawn kite signature is only the first of these, $\sigma(\mathsf{K1}) = \{(0, \frac{3}{4})\}$: the notch segment is not part of the kite's decoration (Remark 2.9), yet the geometry carries it across the edge. The quotient distinguishes what the coloring cannot: $P(\mathsf{D3}) = \{\mathsf{K1}\}$ while $P(\mathsf{K1}) = \{\mathsf{D3}, \mathsf{K2}\}$, so D3 and K1 present the same colored short edge across a gluing yet lie in different classes. The datum that records the difference is the notch chord, which the drawn decoration places on the dart side alone.

Remark 4.6 (The coarsest detecting datum; the enriched datum is not detecting). Call an edge-local datum $d(s)$ *detecting* if $d(s) = d(s')$ implies $P(s) = P(s')$. Detecting means exactly that the d-partition refines $\Sigma/{\sim}$, so the quotient is, by definition, the coarsest detecting partition.

The implication "detecting ⇒ refines $\Sigma/{\sim}$" is a tracing of the definition of $\sim$ and would hold for the compatibility quotient of any relation whatsoever, decorated or not; it is not a property of $\mathcal{A}$, of Penrose geometry, or of bars. Its content is that the partition is realized by the three-chord assignment $\mathcal{A}$ (Theorem 4.3), not by a construction built for the purpose. The enriched datum of Proposition 3.19 is *not* detecting in this sense: it is a function of length and color pair only (Lemma 3.9(i)), hence constant on $\{\mathsf{D0}, \mathsf{K1}\}$, while $P(\mathsf{D0}) = \{\mathsf{K2}\} \neq \{\mathsf{D3}, \mathsf{K2}\} = P(\mathsf{K1})$. It therefore takes only the four values (3.5) and realizes the coloring relation, a strict coarsening of $\Sigma/{\sim}$.

Corollary 4.7 (The count cannot detect the quotient; position is essential)**.** *No function of the edge vector and the signed crossing counts detects $\Sigma/{\sim}$. On a single short-edge vector all four short classes occur (already among the one-sided placements of Lemma 3.15), with partner sets* $\{\mathsf{K2}\}$, $\{\mathsf{K1}\}$, $\{\mathsf{D3}, \mathsf{K2}\}$, $\{\mathsf{D0}, \mathsf{K1}\}$ *and partner-set sizes* $1, 1, 2, 2$. *On a single long-edge vector the two long classes occur, with partner sets* $\{\mathsf{D2}, \mathsf{K3}\}$ *and* $\{\mathsf{D1}, \mathsf{K0}\}$*, each of size* 2.

In each display the classes listed share both the edge vector and the crossing vector, by Lemma 3.15(a), while their partner sets differ, so no function of those two data can be detecting. This is the negative half; that the crossing position *supplies what is missing is Theorem 4.3.*

Proof. Immediate from Lemma 3.15 and the partner sets of Table 4.1.

The statement exhibits one witness vector per length class rather than examining all ten edge vectors. One per class suffices: a detecting function must separate every pair of inequivalent classes wherever they occur, so a single vector on which inequivalent classes share the vector and the count already contradicts detection. □

Remark 4.8 (Structure of the quotient). The six classes are organized as (length, color pair) on long edges and (length, color pair, the prototile carrying the half-edge) on short ones. The third bit on short edges is exactly the dart's notch chord of Remark 2.9: inadmissible for the count, indispensable for compatibility.

The asymmetry behind that splitting is visible in the stars of Lemma 3.4*(ii)*: K1 glues to K2 (in the deuce, the king and the queen), while D0 cannot glue to D3—the $432°$ obstruction—so the kite–kite short gluing has no dart–dart analog.

Remark 4.9 (Computational certification). Table 4.1 was checked independently by measurement on a 372-tile patch, within the tolerances recorded in Appendix B. The pipeline measures the crossing incidence without input from (2.1), recording each position by the *nearest* value of the canonical set $\{\frac{1}{4}, \frac{3}{4}, \beta, \gamma\}$ with a rejection threshold. From the kite–dart patch of the Tilings Encyclopedia [HF] we extracted the 372 tiles (238 kites, 134 darts) all of whose vertices carry legal $360°$ stars, assigned integer coordinates in $\mathbb{Z}[\omega]$ to every vertex (zero closure conflicts), and recovered the five Ammann families as the strip boundaries of the pentagrid index, shown in Figure 4.1(a): every family is straight, with the two spacings $\frac{3\varphi+1}{2}$ and $\frac{\varphi+2}{2}$ in Fibonacci-word order. The measured crossings agree with the signature of Table 4.1 on all 134 dart edges of each of the four classes and on $235/238$ long kite edges of each class, the three exceptions per class sitting at the ragged patch boundary (Appendix B).

The short kite edges are the informative case. The drawn signature appears on $90/238$ ($\mathsf{K1}$) and $89/238$ ($\mathsf{K2}$); the remaining 148 and 149 carry exactly one extra crossing, at $(2, \beta)$ on $\mathsf{K1}$ and $(3, \gamma)$ on $\mathsf{K2}$. These extras are not noise but geometry: the notch segment's endpoints lie on the dart's short edges, so across the legal pairings $\mathsf{D3}|\mathsf{K1}$ and $\mathsf{D0}|\mathsf{K2}$ (observed 128 times each) the kite half-edge necessarily registers the same physical crossing, mirrored (Remark 2.9), and the remaining 20 ($\mathsf{K1}$) and 21 ($\mathsf{K2}$) lie on unglued boundary short edges crossed by the continuations of the same notch lines. The three-chord assignment draws the segment on the dart only, while the Ammann line continues across the kite near the vertex: the full line arrangement carries more than the decoration, which is why the signature is defined as the stable part of the measurement.

At every one of the 670 interior gluings the two sides report exactly the same *measured* crossing sets, mirrored by $\tau \mapsto 1 - \tau$; this is a property of the recovered line arrangement and not of $\mathcal{A}$, whose drawn chords do not agree across a dart short edge (Proposition 3.6*(iii)*). The six-class quotient of Table 4.1 is also exactly the quotient computed from the patch's 7 observed gluing pairs, which are precisely the realizable pairs of Lemma 3.4*(i)*. The signature table is thus verified by two independent tracks: the symbolic evaluation of Appendix A, itself machine-checked in exact $\mathbb{Q}(\sqrt{5})$ arithmetic, and the present patch measurement. The patch is a single finite patch, and nothing is claimed beyond it. The classification is unchanged when the two pipeline tolerances vary over the ranges recorded in Appendix B.

Remark 4.10 (Relation to Minnick's tabulated distances). Minnick's Table 3.1 [Min98] tabulates, from the classical figures, the distances from the prototile vertices to the Ammann lines. Her values are those of the present paper in un-normalized form: the short-edge crossings at 0.25 and 0.75 on unit edges (our $\frac{1}{4}$ and $\frac{3}{4}$), the long-edge crossing distances 0.309017 and 1.309017 (our $\frac{1}{2\varphi} = \beta\varphi$ and $\frac{\varphi^2}{2} = \gamma\varphi$), the fraction $0.190983 = \beta$ itself, and the dart's notch-line offset $0.059017 = |(2 - \sqrt{5})/4|$ of (2.1). The source is an undergraduate honors thesis and, to our knowledge, its tables were not subsequently published in a refereed venue, so we record the agreement as a historical antecedent of bar-to-tile distance tables, not as part of the verification. The verification of Table 4.1 rests on the symbolic derivation of Appendix A and the patch measurement above, both of which are independent of [Min98].

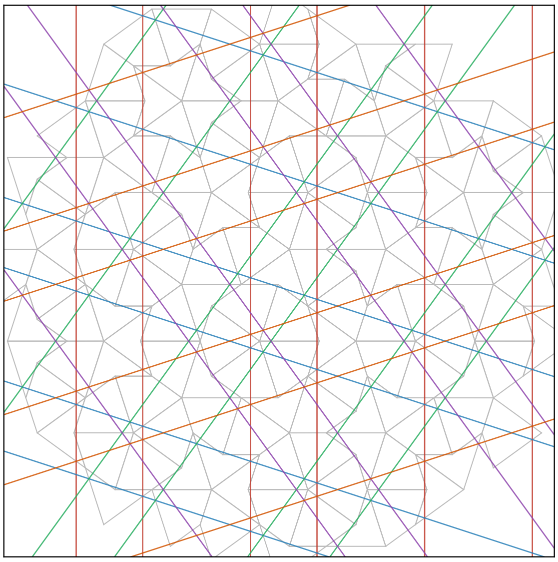

(a) Ammann bars join across tiles

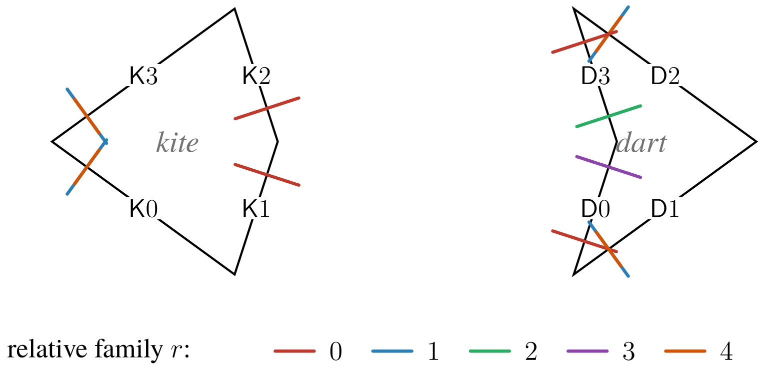

(b) crossing signature ticks per intrinsic edge

Figure 4.1: (a) The five Ammann families on a patch of the valid tiling: each family is straight, and the lines join across tiles. (b) The crossing ticks of Table 4.1 on the reference kite and dart, at the exact fractions $\frac{1}{4}$, $\frac{3}{4}$ and $\beta = \frac{3-\sqrt{5}}{4}$, $\gamma = \frac{1+\sqrt{5}}{4}$: solid ticks are the perpendicular chords $(0, \frac{1}{4})$, $(0, \frac{3}{4})$ and the doubled long-edge crossings at β, γ (nested ticks: the two crossings coincide). The dart's short edges carry in addition the notch chord (relative families 3 on D0, 2 on D3), which separates the dart short classes from the kite's. Tick color records the relative bar family $r \in \mathbb{Z}_5$. The color key is $r = 0$, $r = 1$, $r = 2$, $r = 3$, $r = 4$. The tick values, class by class, are the six signature rows of Table 4.1; on the long edges the two ticks of a pair sit at one point and are drawn nested. Numerically $\beta = \frac{3-\sqrt{5}}{4} \approx 0.191$ and $\gamma = \frac{1+\sqrt{5}}{4} \approx 0.809$.

5. The Golden Ratio in the Signature

The crossing positions of Theorem 4.3 are not generic reals: all four lie in $\mathbb{Q}(\sqrt{5})$, and the two irrational ones are golden-ratio quantities,

$$\beta = \frac{3-\sqrt{5}}{4} = \frac{1}{2\varphi^2}, \qquad \gamma = \frac{1+\sqrt{5}}{4} = \frac{\varphi}{2}, \qquad \varphi = \frac{1+\sqrt{5}}{2}. \tag{5.1}$$

Neither value is chosen: given the ansatz and the kite offsets of Remark 3.11, the dart's chord lines are forced by cross-edge agreement (Proposition 3.10), and the crossings they determine divide every edge at a rational or golden-ratio point. What is forced is the pair β, γ, not the ansatz that yields them.

Remark 5.1 (Division ratios). A crossing at normalized position τ divides its edge in the ratio $\tau : (1-\tau)$. Ratios are recorded without regard to the order of the two endpoints, the two admissible markings on an edge being exchanged by $\tau \mapsto 1-\tau$. The short-edge crossings $\tau = \frac{1}{4}, \frac{3}{4}$ divide the short edge in the ratio $3:1$. The long-edge crossing $\tau = \gamma = \varphi/2$ divides the long edge in the ratio

$$\frac{\gamma}{1-\gamma} = \frac{\varphi}{2-\varphi} = \varphi^3,$$

using $2 - \varphi = \varphi^{-2}$.

The assignment $\mathcal{A}$ therefore marks on every long edge the point dividing it in the ratio $\varphi^3 : 1$, the cube of the linear inflation factor, and on every short edge the quarter point. On short edges the quarter point is exactly the coloring datum of Lemma 3.9(i). On long edges the division point is the forced coincidence of Proposition 3.10.

Remark 5.2 (A scale-comparison reading of the division ratios). This remark is expository and enters no proof. The ratios collected in this section can be compared on a common scale. Let

$$J(x) = \tfrac{1}{2}\big(x + x^{-1}\big) - 1 = \cosh(\ln x) - 1, \qquad x > 0,$$

the *reciprocal-invariant scale-comparison cost* [PGTSW26, PGWA26, WZ26, WZA26]: symmetric under $x \mapsto x^{-1}$, vanishing only at $x = 1$, and a solution of the d'Alembert functional equation

$$J(xy) + J(x/y) = 2\big(J(x)+1\big)\big(J(y)+1\big) - 2 \tag{5.2}$$

[Acz66]. The hypotheses under which (5.2) determines J uniquely, namely a regularity assumption and a calibration on top of the equation itself, are standard material and are recorded as Remark C.6 in Appendix C. The present remark uses none of this: it uses only the closed form of J and the evaluations below. On the constants of this section J evaluates in closed form: $J(3) = \frac{2}{3}$ for the short-edge division ratio, $J(\varphi) = \frac{\sqrt{5}-2}{2}$ for the inflation factor, which is also the ratio of the two bar spacings, $J(\varphi^2) = \frac{1}{2}$ for the reciprocal $1/(2\beta) = \varphi^2$ of the doubled signature fraction, and $J(\varphi^3) = \sqrt{5} - 1$ for the long-edge division ratio.

For comparison, the two other classical quasiperiodic systems carrying bar decorations are the Ammann–Beenker octagonal system, of inflation multiplier $1 + \sqrt{2}$, and the dodecagonal system, of multiplier $2+\sqrt{3}$ [BG13, Ch. 6], and on these J takes the values $J(1+\sqrt{2}) = \sqrt{2}-1$

and $J(2+\sqrt{3}) = 1$. Since J is strictly increasing on $(1,\infty)$ the resulting order carries no information beyond $\varphi < 1+\sqrt{2} < 2+\sqrt{3}$.

What the values add to the bare order is the size of the separation on a common scale: $J(\varphi) = \frac{\sqrt{5}-2}{2} \approx 0.118$, against $\sqrt{2}-1 \approx 0.414$ and 1.

6. Discussion

Five questions are left open, and the five paragraphs below take them in turn: the reach of the half-edge and gluing construction beyond the Penrose family; the P2 analogue of de Bruijn's duality theorem; the effect of lengthening the context; a characterization of which finite-range matching rules admit an edge-local positional signature realizing their compatibility quotient; and the behavior of the quotient under inflation. Of these the first and the fourth are the principal ones, the remaining three being specific to the present construction. A sixth paragraph records the grade of verification the results carry; it raises no question and is included because the distinction between symbolic proof and patch measurement runs through the paper.

All but the duality question presuppose what this paper supplies for P2: the quotient of a concrete rule, computed together with a drawn decoration realizing it. With that step available, the two-part question, compute the quotient and then ask for a positional realization, is well posed for every finite-range rule.

Scope within the Penrose family and beyond. The results are stated for P2 (dart–kite). P3 has the same five-bar structure [GS87, §10.6], but the rhombus arrow decoration refines the geometric half-edge states, so we do not assert the transfer: computing the P3 compatibility quotient and its signature is a separate verification we leave open. P1 likewise requires separate verification [BG13, Ch. 6]. Further natural targets are the classical Ammann aperiodic sets [AGS92], where local rules are known to exist, the Ammann-bar decorations constructed for octagonal systems in [FP24], and the rhombic systems analyzed through weak local rules [BF15, FL24]. In each of these the two-part question transfers even though the P2 answers do not. The metatile matching rules of the hat and Spectre monotiles [SMKGS24a, SMKGS24b] are a further target, but not an immediate one. Their rules are hierarchical rather than edge-to-edge, so Definition C.1 does not apply to them as stated, and the first step would be to present the rules as a finite-range edge-matching rule on marked prototiles. Their compatibility quotient, in any such presentation, is uncomputed.

Open problem (P2 pentagrid duality). De Bruijn's duality theorem [dB81] is proved for the rhombus (P3) tilings. The bar recovery of Appendix B computes the strip boundaries of the pentagrid index on a P2 patch and identifies the resulting straight five-family grid with the classical Ammann bars only empirically (Remark 2.7). The open problem is to construct the P2 analogue: a theorem identifying the strip-boundary grid of a kite–dart tiling with its classical Ammann grid, for instance through the standard P2–P3 mutual local derivability. Its resolution would convert the empirical identification into a theorem. No result of §3–§4 depends on it: the theorems concern the explicit assignment $\mathcal{A}$, and the certification checks of Appendix B are internal to the recovered grid.

Open problem (the context-length hierarchy). The equivalence of §4 compares half-edge classes by their legal partners across a single edge, so the partition computed here is the *one-*

step quotient, in the sense of the covers recalled in §1.2. Lengthening the context can only refine it. For $r \geqslant 1$ let $s \sim_r s'$ hold when the two classes admit the same set of legal patches of radius r containing the glued edge, so that $\sim_1$ is the relation $\sim$ of this paper and $\sim_1 \supseteq \sim_2 \supseteq \cdots$. Being a decreasing chain of partitions of an eight-element set, it stabilizes at some finite r. The open problem is to compute where: whether $\sim_2$ already differs from $\sim_1$, and what the stable partition is. Two outcomes are of unequal interest. Should the chain stabilize at $r = 1$, the six classes of Proposition 4.1 are the whole edge-local content of the rule at every radius, and Theorem 4.3 exhibits a drawn datum carrying all of it. Should it refine, each refinement step is a finite quantity of additional information that a drawn decoration would have to supply, and the question of which decoration supplies it reopens at each level. We have not computed $\sim_2$ and do not conjecture which outcome holds.

Open problem (which rules admit a drawn realization). The four-class coloring relation of Lemma 3.9 records what an edge presents to its neighbor. The six-class quotient records the partners a half-edge can legally meet. That a purely positional datum can carry the detecting content of a matching rule raises the inverse question: given a finite signature table, when does a chord decoration exist that realizes it? Already for P2 the table is constrained: the positions lie in $\mathbb{Q}(\sqrt{5})$ and the families are relative to the edge direction, so a realizing decoration must satisfy the cross-edge agreement equations of Proposition 3.10. Whether such equations admit solutions for a given table is the open content.

Open problem (behavior under inflation). The remaining question is whether the six-class quotient survives the passage to the cartwheel inflation [GS87, §10.3]: is the compatibility partition of a supertile level a function of the level below?

An affirmative answer is plausible on structural grounds, though we do not claim it follows from them: inflation carries legal gluings to legal gluings and preserves the Ammann bars [GS87, §10.6], so the data on which a supertile side's partner set could depend are present at the level below. That is a reason to look, not a proof that the dependence exists. Where to look can be said precisely. The relevant datum is the inflated chord data and not the substitution matrix, since the matrix records how many kites and darts a supertile contains, which is frequency information and says nothing about which half-edge classes a supertile side presents, whereas the quotient depends only on the latter. Concretely, one computes the signature that a supertile side inherits from the chords of $\mathcal{A}$ crossing it, in the sense of Definition 4.2 applied one level up. Should that signature again take six values, the quotient is preserved, and the further question is whether the induced map on classes is the identity or a nontrivial permutation. We assert neither, and the computation has not been carried out.

Verification grade. The logical core of §4 is well suited to machine-checked verification: the quotient is a finite enumeration over eight classes and thirty-two ordered pairs, and the signature table is a finite list of elements of $\mathbb{Q}(\sqrt{5})$, a field with a faithful and decidable arithmetic. Neither step involves a limit, a compactness argument, or an appeal to a geometric picture, so Proposition 4.1 and Theorem 4.3 could in principle be reduced to a kernel-checked computation in a proof assistant. We have not carried this out. The classical inputs would remain outside such a formalization, in particular the three-chord ansatz and the kite offsets of Remark 3.11, so a formalization would certify the combinatorial and arithmetic content of the theorems and not their agreement with the classical Ammann decoration.

7. Conclusion

This paper has determined what one side of an edge in a Penrose kite–dart tiling knows about the other side. The one-sided content of the rule is the compatibility quotient, the Myhill–Nerode quotient of the rule on its eight half-edge classes, formed from the fourteen realizable legal ordered pairings. It has exactly six classes. Although its definition mentions no decoration, the quotient is realized exactly by a drawn datum. The three-chord assignment $\mathcal{A}$, read on each half-edge as the relative bar family and the normalized position of each chord crossing, takes six distinct values, one per class. Its identification with the stable part of the classical Ammann decoration is empirical and single-patch (Remark 2.7). Every theorem concerns $\mathcal{A}$ itself. By the definition of the quotient, no coarser edge-local datum can detect the rule.

Three items in this analysis are, to our knowledge, new. First, the compatibility quotient of the P2 matching rule had not been computed before: the six-class partition of Table 4.1 and its partner sets appear here for the first time. Second, no previous work had identified a decoration drawn on the tiles whose edge data realize such a quotient exactly; the classical literature uses the Ammann bars to characterize global validity, not to encode the partner structure of the rule. Third, the separation between the two components of the crossing datum, the count being a function of the edge vector alone while the position carries all the detecting content, had not been stated or proved. The count half is an elementary enumeration (Lemma 3.15), but that it is sharp is not: the kite-plus-dart rhombus tiles the plane periodically with all five count conditions satisfied and the matching rule failing at asymptotically half of its interior edges (Proposition 3.17). The motivation for all three is the same question: how much of an aperiodic matching rule is visible from one side of a single edge. The quotient is the exact answer, and $\mathcal{A}$ is a decoration that draws it. Within the three-chord ansatz the dart's offsets are forced rather than selected (Proposition 3.10). Agreement of the crossing position edge by edge is equivalent to the matching rule, and the positions themselves are golden-ratio quantities, dividing each long edge in the ratio $\varphi^3 : 1$ and each short edge in the ratio $3 : 1$.

The computations are of two kinds, and the results rest on the first. The signature table and the crossing vectors of Table 2.1 are derived symbolically in $\mathbb{Q}(\sqrt{5})$, with no floating-point operation, and this is what proves Theorem 4.3. The 372-tile patch check of Appendix B, which reads floating-point coordinates and quantizes them within stated tolerances, corroborates the derivation rather than establishing it. What the construction adds is a reading of the matching rule from one side of each edge, and a benchmark, the compatibility quotient, against which every edge-local datum, drawn or not, can be measured.

Data Availability Statement

The certification scripts and the extracted clean-patch data described in Appendix B are included as ancillary files with this article. The source kite–dart patch is distributed by the Tilings Encyclopedia [HF].

The bundle is pinned so that a rerun can be checked against the published run rather than against a later revision. It contains sixteen files, and a manifest `SHA256SUMS` listing the SHA-256 digest of each; that manifest has digest

`8c5e2822df2a67274e16f7d49af7f024c56d592004b616cf4f347c3d7415107d.`

The patch coordinate file `kd_clean.txt`, from which every number quoted in Remark 4.9 is derived, has digest

`6a115e3ad4a4b2c07787232825da21b6c894659fec820a03cfcb1b37c510b966.`

All numbers reported here come from a single run under CPython 3.11.9 on Windows; the per-script dependencies are listed in `requirements.txt`.

One command regenerates every computed number in the paper: `python reproduce.py` runs the three independent generators of Appendix B in turn and prints a single verdict, and each may also be run alone. The two symbolic stages evaluate the offsets (2.1) by exact arithmetic in $\mathbb{Q}(\sqrt{5})$; the patch stage measures within the tolerances of Appendix B and is corroborative rather than probative.

A. The Signature Table in $\mathbb{Q}(\sqrt{5})$

We carry out the finite computation on which Theorem 4.3 rests: the evaluation of the three-chord assignment $\mathcal{A}$ (2.1) on the reference prototiles of Definition 2.6. Everything takes place in $\mathbb{Q}(\sqrt{5})$: writing $\zeta = e^{2\pi i/5}$ and $\mathbf{n}_i = \zeta^i$ (so that $\mathbf{n}_i{\cdot}x = \mathrm{Re}(\zeta^{-i}x)$), every vertex of the reference placement is an integer combination of the ζ^l, and $\mathbf{n}_i{\cdot}\zeta^l = \cos\big(72°(l-i)\big)$ takes only the three values

$$1, \qquad \cos 72° = \tfrac{\sqrt{5}-1}{4}, \qquad \cos 144° = -\tfrac{\sqrt{5}+1}{4}.$$

The vertex projections needed below are therefore exact, and are collected in Table A.1.

Table A.1: Projections $\mathbf{n}_i \cdot v$ of the reference vertices (Definition 2.6) on the chord families drawn by each prototile. Two abbreviations suffice, $\lambda = \frac{\sqrt{5}-1}{4}$ and $\nu = \frac{3+\sqrt{5}}{4} = \lambda + 1$, since the remaining two values that occur are $-\lambda$ and $\gamma = \frac{1+\sqrt{5}}{4} = \lambda + \frac{1}{2}$, the latter already one of the four crossing positions of (3.5). Every entry of the table therefore lies in $\{0, \pm\frac{1}{2}, \pm 1, \pm\lambda, \nu, \gamma, \varphi\}$.

	kite: X, Z', Y, Z				dart: X, Z', Y, Z			
family	X	Z'	Y	Z	X	Z'	Y	Z
$\mathbf{n}_0$	0	ν	$\frac{1+\sqrt{5}}{2}$	ν	0	$-\lambda$	1	$-\lambda$
$\mathbf{n}_1$	0	$-\frac{1}{2}$	$\frac{1}{2}$	ν	0	-1	λ	γ
$\mathbf{n}_4$	0	ν	$\frac{1}{2}$	$-\frac{1}{2}$	0	γ	λ	-1

A chord $\mathbf{n}_i{\cdot}x = c$ meets the directed edge $a \to b$ if and only if $(\mathbf{n}_i{\cdot}a - c)\,(\mathbf{n}_i{\cdot}b - c) < 0$, and then the normalized crossing position is $\tau = (c - \mathbf{n}_i{\cdot}a)/\big(\mathbf{n}_i{\cdot}(b-a)\big)$. The edge vectors of the reference placement are $1+\zeta^4, \zeta, 1+\zeta-\varphi, -1-\zeta$ on the kite and $-\zeta, 1+\zeta, -1-\zeta^4, \zeta^4$ on the dart, of directions ω^j or $\varphi\,\omega^j$ with $j = 9, 2, 3, 6$ and $j = 7, 1, 4, 8$ respectively; the relative family of a family-i chord is $r \equiv 2i - j \pmod 5$. We give two sample evaluations; the remaining ones are identical in form. On $\mathsf{K}0$ ($X \to Z'$, $j = 9$) the family-0 chord meets the edge at

$$\tau = \frac{\frac{1}{4} - 0}{\nu - 0} = \frac{1}{3+\sqrt{5}} = \frac{3-\sqrt{5}}{4} = \beta, \qquad r \equiv 0 - 9 \equiv 1 \pmod 5;$$

the family-1 chord does not meet it ($\mathbf{n}_1 \cdot X = 0$ and $\mathbf{n}_1 \cdot Z' = -\frac{1}{2}$ are both $< \frac{1}{4}$), and the family-4 chord repeats the family-0 computation with $r \equiv 8 - 9 \equiv 4$. On D3 ($Z \to X$, $j = 8$) the family-0 notch chord, at offset $\frac{2-\sqrt{5}}{4}$, meets the edge at

$$\tau = \frac{\frac{2-\sqrt{5}}{4} - (-\lambda)}{0 - (-\lambda)} = \frac{\frac{1}{4}}{\lambda} = \frac{1}{\sqrt{5}-1} = \frac{1+\sqrt{5}}{4} = \gamma, \qquad r \equiv 0 - 8 \equiv 2 \pmod{5},$$

and the family-4 chord gives $\tau = \frac{1}{4}$, $r \equiv 0$. The complete evaluation is given in Table A.2.

Table A.2: The complete evaluation of the three-chord assignment $\mathcal{A}$ (2.1) on the eight half-edge classes of the reference prototiles. Each row lists the chord families meeting the edge, the pairs (r, τ) they contribute, and the resulting three-chord signature of Definition 4.2. The six distinct signatures are the last column of Table 4.1.

edge	chord families met	(r, τ)	signature
K0	$0, 4$	$(1, \beta), (4, \beta)$	$\{(1, \beta), (4, \beta)\}$
K1	1	$(0, \frac{3}{4})$	$\{(0, \frac{3}{4})\}$
K2	4	$(0, \frac{1}{4})$	$\{(0, \frac{1}{4})\}$
K3	$0, 1$	$(4, \gamma), (1, \gamma)$	$\{(1, \gamma), (4, \gamma)\}$
D0	$1, 0$	$(0, \frac{3}{4}), (3, \beta)$	$\{(0, \frac{3}{4}), (3, \beta)\}$
D1	$1, 0$	$(1, \beta), (4, \beta)$	$\{(1, \beta), (4, \beta)\}$
D2	$4, 0$	$(4, \gamma), (1, \gamma)$	$\{(1, \gamma), (4, \gamma)\}$
D3	$4, 0$	$(0, \frac{1}{4}), (2, \gamma)$	$\{(0, \frac{1}{4}), (2, \gamma)\}$

Reading the rows of Table A.2 together gives the six distinct values of Table 4.1: the long rows K0 $=$ D1 and K3 $=$ D2 are doubled pairs at the *same* crossing point, and on the short rows the notch chord appears exactly on the dart, at relative family 3 on D0 and 2 on D3. With the projections of Table A.1 and the two sample evaluations above, every row can be checked by hand, so this appendix is verifiable without running any of the ancillary code.

B. Computational Certification

We describe the pipeline behind Remark 4.9 and the machine checks of Appendix A. All scripts and the extracted patch data are included as ancillary files; every number quoted in Remark 4.9 is the output of a single run of the pipeline described below.

Source and legality filter. The kite–dart substitution patch of the Tilings Encyclopedia [HF] is distributed as a vector graphic; tile polygons are read directly from its path stream and deduplicated by vertex set (8898 unique tiles), with edge lengths normalized so the short edge is 1. A vertex is *legal* if the corner angles of its incident tiles sum to 360° (tolerance 0.5°); every legal vertex of the patch realizes one of the seven stars of Lemma 3.4*(ii)*. Legality is enforced in two stages. The extraction script keeps the tiles whose four vertices are all legal in the full deduplicated set (3266 tiles), certifies by a pairwise winding-number check that the kept tiles overlap nowhere, and pins the result as `kd_clean.txt`. At each run the certification driver recomputes legality within the pinned set, incident tiles drawn only from that set, and keeps the tiles whose four vertices remain legal. These form the *clean patch*: 372 tiles (238 kites, 134 darts). Its boundary is ragged, which is why legality is enforced vertex by vertex rather than by radius.

Integer coordinates. Each vertex is assigned a vector in $\mathbb{Z}[\omega]$, $\omega = e^{i\pi/5}$, by propagation from a base vertex: crossing a short edge adds a unit power $\pm\omega^j$ and crossing a long edge adds $\pm\varphi\,\omega^j$, the sign and j read from the measured displacement rounded to the nearest element of $\{\omega^j, \varphi\,\omega^j\}$ (the largest rounding error over the 1488 tile-edge incidences of the clean patch is 2.1×10^{-3}, against a separation of $2\sin 18^\circ \approx 0.62$ between adjacent edge directions, so the rounded element is always the correct one). Around every cycle of the patch the assignments close with zero conflicts, so the coordinates are exact; in particular every vertex lies in $\mathbb{Z}[\omega]$ and every edge displacement has the asserted form. The index vector $k(v) \in \mathbb{Z}^5$ is de Bruijn's pentagrid index [dB81]: the five coordinates of v in the generating set $\{\omega^{2i}\}$ modulo the diagonal (the relation $\sum_i \omega^{2i} = 0$ of Lemma C.2).

Bar recovery. For each family i the vertices are grouped by the strip level $s_i(k) = k_i - \frac{1}{5}\sum_l k_l$. Wherever two consecutive levels are strictly separated—the largest projection of one level smaller than the smallest projection of the next—a candidate bar line is placed at the midpoint of the gap; every candidate gap has clearance $\geqslant 0.49$. Over the interior of the patch the candidates of each family form a single run whose consecutive spacings take exactly the two values $\frac{\varphi+2}{2}$ and $\frac{3\varphi+1}{2}$, the short–long order a factor of the Fibonacci word (12 to 18 bars per family). At the ragged corners of the patch the strip levels fragment and a few isolated spurious candidates appear (at most five per family, all outside the run's span); these are excluded from the spacing check but retained for the measurement below, where their only effect is the three boundary artifacts per long-kite class (six in total) of Remark 4.9. The recovered lines are straight by construction, and they form a five-family grid with the two classical spacings in Fibonacci-word order; the identification of this grid with the classical Ammann bars is discussed, with its empirical status, in Remark 2.7, and is stated as a named open problem in §6.

Every check of this appendix is a statement about the recovered grid itself and holds independently of that identification, which is needed only to call the grid the Ammann grid and enters no check.

Signature measurement. Each tile is rotated to its intrinsic canonical position (dart: boundary from the reflex vertex; kite: from the vertex opposite the 144° vertex; counterclockwise in both cases), so its four edges are labeled $\mathsf{K}0, \ldots, \mathsf{D}3$ of Definition 3.3. For every edge the crossing by every recovered bar line is recorded as the pair (r, τ) of Definition 4.2; τ is snapped to the nearest value of the canonical set $\{\frac{1}{4}, \frac{3}{4}, \beta, \gamma\}$ and rejected if its distance to that nearest value exceeds 0.03 (nearest-first, so the overlap of the β and $\frac{1}{4}$ windows creates no ambiguity), and crossings with $\tau < 0.06$ or $\tau > 0.94$ (near-vertex continuations) are discarded.

Tolerance sensitivity. The two tolerances are overridable at run time (environment variables `TOL_POS` and `TOL_VERT` of `certify.py`), and the full check suite passes unchanged for `TOL_POS` in $[0.01, 0.05]$ and `TOL_VERT` in $[0.1^\circ, 2^\circ]$. The measured deviations explain the margins: over all crossings encountered on the clean patch, every genuine crossing deviates from its canonical value by less than 0.01 (median 5×10^{-4}), the ten off-canonical boundary crossings deviate by more than 0.059, and the band $(0.01, 0.059)$ is empty, so every tolerance inside that band produces the identical classification. Below 0.01 the suite fails only because eight genuine crossings with deviations in $(0.005, 0.01)$ are then discarded. Per class the observed patterns and multiplicities match the signature of Table 4.1: constant on all 134 dart edges of each class and on $235/238$ long kite edges of each class; the drawn signature on $90 + 89$ short kite edges, with the notch-line continuation as the unique extra crossing on the remaining $148 + 149$.

Checks. (i) Join consistency: at each of the 670 interior gluings the two half-edges report the same crossing set, mirrored by $\tau \mapsto 1 - \tau$ (the relative family $r = (2i - j) \bmod 5$ is invariant under edge reversal, since $j \mapsto j + 5$); $670/670$ agree exactly. (ii) The patch's 7 unordered gluing pairs are exactly the realizable pairs of Lemma 3.4*(i)*, and the partner-set partition of the eight classes computed from them is the six-class quotient of Table 4.1. (iii) The evaluation of Appendix A is reproduced symbolically (exact arithmetic in $\mathbb{Q}(\sqrt{5})$, all twenty-four chord–edge pairs), confirming each entry of Table 4.1, including the doubled long-edge crossings and the notch-chord positions β, γ.

Artifacts. Ancillary files (with a `README`): the one-command driver `reproduce.py`; the certification driver `certify.py`; the extraction and filtering scripts `pdf_tiles.py`, `clean_patch.py`; the coordinate, bar, and canonicalization modules `coords.py`, `bars.py`, `canon.py`; `symbolic_table.py` for the symbolic evaluation of Appendix A and `crossing_vectors.py` for that of Table 2.1; the figure script `make_figure.py` with its outputs `fig_ammann.pdf` and `fig_ammann.png`; the dependency list `requirements.txt`; the source patch `kd_patch.pdf`; and the pinned patch data `kd_clean.txt` (the 3266 legal-vertex tiles, from which the 372-tile clean patch is extracted at each run).

A single run of `reproduce.py` regenerates every computed number in the paper and ends with `ALL STAGES PASS`; the patch stage alone, `certify.py`, reproduces every number quoted in Remark 4.9 and ends with `ALL CHECKS PASSED`. Both run from any directory.

`certify.py` uses the standard library only; `symbolic_table.py` requires `sympy`, and `make_figure.py` requires `matplotlib` and `numpy`. The scripts are short, single-purpose, and included in full; the claims of this appendix are checkable only against those ancillary files, not from the manuscript alone.

Every number quoted in this appendix appears verbatim in the output of one of three scripts: the extraction counts 8898 and 3266 in that of `clean_patch.py`, the patch measurements and checks (i) and (ii) in that of `certify.py`, and the exact evaluations of check (iii) in that of `symbolic_table.py`.

C. General definitions and elementary material

This appendix records six items moved out of the main text: the compatibility quotient of an arbitrary finite-range edge-matching rule, of which §4 uses only the P2 instantiation (Definition C.1); a standard cyclotomic lemma (Lemma C.2); two elementary observations in plane geometry that explain why a pair of natural arguments fail (Remarks C.3 and C.4); the reflection invariance of the P2 decorations, verified in coordinates (Remark C.5); and the classical uniqueness discussion for the cost function of Remark 5.2 (Remark C.6). All six are elementary or standard. Only Lemma C.2 is used in the main text, and there only by citation, in Remark 2.12; the other five support the exposition without entering a proof.

Definition C.1 (The compatibility quotient of an edge-matching rule)**.** Let $\mathcal{P}$ be a finite set of marked prototiles and R a finite-range edge-matching rule: a symmetric relation on the finite set Σ of *half-edge classes*—(prototile, edge, mark) triples up to orientation-preserving rigid motion, the edge directed counterclockwise around the prototile—where $s|s'$ records that an edge of class s may be glued, oppositely traversed, to an edge of class s'. The *partner set* of s is $P(s) = \{s' \in \Sigma : s|s'$ holds and occurs in some R-tiling$\}$, and s, s' are *compatible-equivalent*, $s \sim s'$, if $P(s) = P(s')$. The quotient $\Sigma/{\sim}$ is the *compatibility quotient* of the rule. The terminology is the Myhill–Nerode equivalence of formal language theory [Myh57, Ner58, HU79], read off the one-step transition structure of the rule: two half-edge classes are identified when they have the same right context. A *signature* for the rule is any edge-local datum constant on classes. It *realizes* the quotient if equality of signatures is equivalence. The quotient is intrinsic to the rule—it mentions no decoration—while a realizing signature is a concrete representative, and the question of which rules admit one drawn on the tiles is the content of the open problems in §6.

The clause "and occurs in some R-tiling" in the definition of $P(s)$ is a substantive convention, not a technicality, and two consequences of adopting it should be recorded. First, the P2 quotient depends on it. Were $P(s)$ taken to be the set of merely mark-legal partners, the pair D0|D3 would be admitted—it is excluded by the $432°$ angle count at the far endpoint of the glued edge (Lemma 3.4*(i)*), which is not a consequence of the mark-matching relation R and is not visible at the vertex being examined, though it is local—and then $P(\mathsf{D0}) = \{\mathsf{D3}, \mathsf{K2}\} = P(\mathsf{K1})$, collapsing the six classes of Proposition 4.1 onto the four coloring classes. The separation of the dart's short classes from the kite's is therefore produced by the occurrence convention together with the classical vertex-star classification (Lemma 3.4), and not by the local relation R alone. Second, for a general finite-range rule the occurrence predicate need not be decidable, undecidability already being available for small tile sets [Rob71, DL25, Sta25], so $\Sigma/{\sim}$ as defined here need not be computable from R by any uniform procedure. For P2 it is computable because the vertex-star classification is known and finite.

Lemma C.2 (The relation module of the five bar directions)**.** $\{\, c \in \mathbb{Z}^5 : \sum_{k=0}^{4} c_k \mathbf{n}_k = \mathbf{0} \,\} = \mathbb{Z} \cdot (1,1,1,1,1)$.

Proof. Identify $\mathbb{R}^2 \cong \mathbb{C}$ and $\mathbf{n}_k \leftrightarrow \zeta^k$, $\zeta = e^{2\pi i/5}$. Then $\sum_k c_k \mathbf{n}_k = \mathbf{0}$ says the integer polynomial $p(x) = \sum_{k=0}^{4} c_k x^k$, of degree at most 4, vanishes at ζ, so p is divisible in $\mathbb{Q}[x]$ by the minimal polynomial $\Phi_5(x) = 1 + x + x^2 + x^3 + x^4$ of ζ, with integer quotient by Gauss's lemma. Comparing degrees, $p = m\Phi_5$, i.e. $c = m\,(1,1,1,1,1)$ with $m \in \mathbb{Z}$. The converse is $\sum_k \zeta^k = 0$. $\square$

The lemma is a standard consequence of the irreducibility of Φ_5 over $\mathbb{Q}$ [Was97, Ch. 1], and is numbered here only so that Remark 2.12 and Appendix B can cite it.

The next two remarks are moved verbatim from §2.4. The first explains why the parity statement of Remark 2.5(iii) is stated per chord rather than per family. The second explains why the P3 correspondence between bar families and edge-direction classes has no P2 analogue, which is what makes Lemma 2.11 necessary.

Remark C.3 (Why parity is a decoration fact, not a transversality fact). Deriving (iii) from Remark 2.5(i) alone, on the ground that a bar entering a tile must leave it, gives evenness but not the bound 0 or 2, and the appeal to convexity is unavailable: the dart has a reflex vertex of $216°$. For the dart with $v_0 = (0, 0)$, $v_1 = (\varphi, 0)$, long edges $\overline{v_0 v_1}$, $\overline{v_1 v_2}$ and short edges $\overline{v_2 v_3}$, $\overline{v_3 v_0}$, a line in the bar direction $54°$, one of the five realizable bar directions for this placement, meets *all four* edges for every offset in an interval of length $\cos 72° = \frac{1}{2\varphi} = \frac{\sqrt{5}-1}{4} \approx 0.3090$, cutting the two wings in two separate chords. Parity survives, 4 being even and each chord contributing $+1$ and -1. The sharper count 0 or 2 per family does not, which is why (iii) is stated per chord. That the decoration does place a dart bar in that interval (Remark 2.8) is a decoration fact, not a transversality one.

Remark C.4 (Why there is no "one family per edge-direction class" rule for P2). The bijection between the five bar families and the five edge-direction classes is a *P3* fact: each rhombus has two parallel edges per class, one family is nonzero on them, and they contribute $+1$ and -1. For P2 the analog—every edge of a class crossed by its associated family, the tile-side value always ± 1 and never 0—is false. Neither P2 prototile has a pair of parallel edges: the kite has interior angles $72°, 72°, 144°, 72°$ and the dart $72°, 36°, 216°, 36°$, both with cyclic edge pattern (long, short, short, long), so the four edges fall into *four distinct* line-direction classes with exactly *one* edge in each. Such a rule would contribute exactly one nonzero term, of value ± 1, to the oriented boundary sum of that family. Every per-family boundary sum vanishes, however, each chord entering and leaving the tile once. What *enriched gluing* $\Rightarrow$ *matching* in Lemma 3.9(iii) needs in its place is Lemma 2.11, every edge being crossed by at least one family: parity alone would permit an edge on which *all five* values vanish for both admissible markings, where the gluing conditions read $0 = 0$.

Remark C.5 (Reflection invariance of the P2 decorations, in coordinates). This remark verifies the statement of Remark 2.2, that both prototiles are mirror-symmetric about the axis joining their two axial vertices and that their decorations are invariant under that reflection. For the Ammann bars this is visible in (2.1): the axial reflection is complex conjugation, which sends family f to family $-f$ and hence exchanges families $1 \leftrightarrow 4$ and $2 \leftrightarrow 3$ while fixing family 0. The bar set is therefore reflection-invariant exactly when the family-1 and family-4 offsets agree, and they do, on both prototiles ($\frac{1}{4} = \frac{1}{4}$ for the kite, $-\frac{3}{4} = -\frac{3}{4}$ for the dart). For the vertex coloring of Definition 3.3 it is immediate and needs no computation: the reflection fixes each axial vertex and exchanges the two wings, and the two wings carry the same color. For the arrows and for Conway's arcs the same argument applies, since each arrow pair and each arc joins a reflection-exchanged pair of edges.

Remark C.6 (Uniqueness of the cost function J). This remark supplements Remark 5.2 and records why the d'Alembert equation (5.2) needs both a regularity hypothesis and a calibration before it pins down J. Setting $x = y = 1$ in (5.2) gives $J(1) \in \{0, -1\}$, so nonnegativity forces $J(1) = 0$; the normalization is a consequence of (5.2), not an independent hypothesis. Equation

(5.2) does not by itself determine J: the one-parameter family $J_c(x) = \cosh(c \ln x) - 1$ satisfies (5.2) for every $c > 0$, since $\cosh\big(c\ln(xy)\big) + \cosh\big(c\ln(x/y)\big) = 2\cosh(c\ln x)\cosh(c\ln y)$. Nor does a calibration suffice on its own. Without a regularity hypothesis (5.2) admits pathological, non-measurable solutions, exactly as Cauchy's equation does, and an evaluation at one point cannot exclude them. The two hypotheses do separate work, and it is the regularity that confines the solutions to a one-parameter family. In the logarithmic variable $H(t) = J(e^t) + 1$, equation (5.2) becomes d'Alembert's equation

$$H(t+s) + H(t-s) = 2H(t)H(s), \qquad t, s \in \mathbb{R}, \tag{C.1}$$

whose *continuous* solutions are classically $H \equiv 0$, $H(t) = \cos(ct)$ and $H(t) = \cosh(ct)$ [Acz66, Ch. 3]. Nonnegativity of J reads $H \geqslant 1$, which discards the first branch, since $H(0) = 1$, and the second, since $\cos(ct) < 1$ for $t \neq 0$ whenever $c \neq 0$. Continuity together with $J \geqslant 0$ therefore forces $J = J_c$ for some $c \geqslant 0$, and only at this stage does a calibration have anything left to determine: $J(2) = \frac{1}{4}$ gives $\cosh(c \ln 2) = \frac{5}{4}$, hence $c \ln 2 = \ln\big(\frac{5}{4} + \frac{3}{4}\big) = \ln 2$ and $c = 1$. Uniqueness of J thus requires all three of (5.2), a regularity hypothesis and a calibration, which is the hypothesis set under which it is proved in [WZ26].

References

[Acz66] J. Aczél. *Lectures on Functional Equations and Their Applications*. Academic Press, 1966.

[AGS92] Robert Ammann, Branko Grünbaum, and G. C. Shephard. Aperiodic tiles. *Discrete Comput. Geom.*, 8:1–25, 1992. doi:10.1007/BF02293033.

[BF15] Nicolas Bédaride and Thomas Fernique. No weak local rules for the $4p$-fold tilings. *Discrete Comput. Geom.*, 54:980–992, 2015. arXiv:1409.0215, doi:10.1007/s00454-015-9740-8.

[BG13] Michael Baake and Uwe Grimm. *Aperiodic Order, Vol. 1: A Mathematical Invitation*. Cambridge University Press, 2013. doi:10.1017/CBO9781139025256.

[BGG25] Michael Baake, Franz Gähler, and Philipp Gohlke. Orbit separation dimension as complexity measure for primitive inflation tilings. *Ergodic Theory Dynam. Systems*, 45(10):2992–3020, 2025. doi:10.1017/etds.2025.18.

[BGMM25] Michael Baake, Franz Gähler, Jan Mazáč, and Andrew R. Mitchell. Diffraction of the Hat and Spectre tilings and some of their relatives. *J. Math. Phys.*, 66(9):092707, 2025. doi:10.1063/5.0264955.

[BGMS25] Michael Baake, Franz Gähler, Jan Mazáč, and Lorenzo Sadun. On the long-range order of the Spectre tilings. *Discrete Comput. Geom.*, 2025. doi:10.1007/s00454-025-00756-z.

[BGS25] Michael Baake, Franz Gähler, and Lorenzo Sadun. Dynamics and topology of the Hat family of tilings. *Israel J. Math.*, 270(1):449–485, 2025. doi:10.1007/s11856-025-2780-8.

[BH23] Michael Baake and Alan Haynes. Convergence of Fourier–Bohr coefficients for regular Euclidean model sets. to appear in Aperiodic Order, Vol. 3, Cambridge Univ. Press, 2023. arXiv:2308.07105.

[BW23] Tinka Bruneau and Michael F. Whittaker. Planar aperiodic tile sets: from Wang tiles to the Hat and Spectre monotiles. *Nieuw Arch. Wiskd. (5)*, 24(4):207–214, 2023. arXiv:2310.06759.

[CGGL26] Thierry Coulbois, Anahí Gajardo, Pierre Guillon, and Victor H. Lutfalla. Aperiodic monotiles: from geometry to groups. *Theoret. Comput. Sci.*, 1059:115555, 2026. doi:10.1016/j.tcs.2025.115555.

[dB81] N. G. de Bruijn. Algebraic theory of Penrose's non-periodic tilings of the plane, I and II. *Nederl. Akad. Wetensch. Indag. Math.*, 43:39–52 and 53–66, 1981. also published as Kon. Nederl. Akad. Wetensch. Proc. Ser. A **84**. doi:10.1016/1385-7258(81)90016-0.

[DL25] Erik D. Demaine and Stefan Langerman. Tiling with three polygons is undecidable. In *41st International Symposium on Computational Geometry (SoCG 2025)*, volume 332 of *LIPIcs*, pages 39:1–39:16, 2025. doi:10.4230/LIPIcs.SoCG.2025.39.

[FGM24] Dirk Frettlöh, Alexey Garber, and Neil Mañibo. Substitution tilings with transcendental inflation factor. *Discrete Anal.*, pages Paper No. 11, 24 pp., 2024. arXiv:2208.01327, doi:10.19086/da.125449.

[Fis75] Roland Fischer. Sofic systems and graphs. *Monatsh. Math.*, 80(3):179–186, 1975. doi:10.1007/BF01319913.

[FL24] Thomas Fernique and V. H. Lutfalla. Geometrical Penrose tilings are characterized by their 1-atlas. *Theoret. Comput. Sci.*, 1022:114883, 2024. arXiv:2211.08239, doi:10.1016/j.tcs.2024.114883.

[FM26] Dirk Frettlöh and Jan Mazáč. Frieze patterns and aperiodic tilings of the plane. *arXiv e-prints*, 2026. arXiv:2607.21348.

[FP24] Thomas Fernique and C. Porrier. Ammann bars for octagonal tilings. *Discrete Math. Theor. Comput. Sci.*, 26(3):#11, 2024. arXiv:2205.13973, doi:10.46298/dmtcs.10764.

[GS87] Branko Grünbaum and G. C. Shephard. *Tilings and Patterns*. W. H. Freeman, New York, 1987.

[GT24] Rachel Greenfeld and Terence Tao. A counterexample to the periodic tiling conjecture. *Ann. of Math. (2)*, 200(1):301–363, 2024. doi:10.4007/annals.2024.200.1.5.

[HF] Edmund Harriss and Dirk Frettlöh. Tilings encyclopedia. https://tilings.math.uni-bielefeld.de/. kite–dart substitution patch.

[HKW25] Edmund Harriss, Henna Koivusalo, and James J. Walton. When is a cut and project set substitutional? *arXiv e-prints*, 2025. arXiv:2512.13659.

[HL25] Alan Haynes and Christopher Lutsko. The Gauss circle problem for Penrose tilings. *arXiv e-prints*, 2025. arXiv:2512.21444.

[HU79] John E. Hopcroft and Jeffrey D. Ullman. *Introduction to Automata Theory, Languages, and Computation*. Addison-Wesley, Reading, MA, 1979.

[JR21] Emmanuel Jeandel and Michael Rao. An aperiodic set of 11 Wang tiles. *Adv. Comb.*, pages Paper No. 1, 37 pp., 2021. arXiv:1506.06492, doi:10.19086/aic.18614.

[Kri84] Wolfgang Krieger. On sofic systems I. *Israel J. Math.*, 48(4):305–330, 1984. doi:10.1007/BF02760631.

[Lev88] L. S. Levitov. Local rules for quasicrystals. *Comm. Math. Phys.*, 119(4):627–666, 1988. doi:10.1007/BF01218348.

[LM95] Douglas Lind and Brian Marcus. *An Introduction to Symbolic Dynamics and Coding*. Cambridge University Press, Cambridge, 1995. doi:10.1017/CBO9780511626302.

[Maz23] Jan Mazáč. Patch frequencies in rhombic Penrose tilings. *Acta Crystallogr. Sect. A*, 79(5):399–411, 2023. doi:10.1107/S2053273323004990.

[Min98] L. Minnick. Generalized forcing in aperiodic tilings. B.a. honors thesis, Williams College, 1998.

[MM26] Juan Marshall-Maldonado. Quantitative weak mixing of self-affine tilings. *Monatsh. Math.*, 209:513–540, 2026. doi:10.1007/s00605-026-02154-w.

[Myh57] John Myhill. Finite automata and the representation of events. Technical Report 57-624, Wright Air Development Center, Wright-Patterson AFB, Ohio, 1957.

[Ner58] Anil Nerode. Linear automaton transformations. *Proc. Amer. Math. Soc.*, 9(4):541–544, 1958. doi:10.1090/S0002-9939-1958-0135681-9.

[Pen74] Roger Penrose. The role of aesthetics in pure and applied mathematical research. *Bull. Inst. Math. Appl.*, 10:266–271, 1974.

[PGTSW26] S. Pardo-Guerra, A. Thapa, M. Simons, and J. Washburn. Coherent comparison as information cost: axiomatic foundations for discrete ledger dynamics. *Foundations*, 6(2):17, 2026. arXiv:2601.12194, doi:10.3390/foundations6020017.

[PGWA26] S. Pardo-Guerra, J. Washburn, and E. Allahyarov. Matching rules as cocycle conditions. 2026. arXiv:2603.13553.

[Rob71] Raphael M. Robinson. Undecidability and nonperiodicity for tilings of the plane. *Invent. Math.*, 12(3):177–209, 1971. doi:10.1007/BF01418780.

[SMKGS24a] David Smith, Joseph Samuel Myers, Craig S. Kaplan, and Chaim Goodman-Strauss. An aperiodic monotile. *Combin. Theory*, 4(1):Paper No. 6, 2024. arXiv:2303.10798, doi:10.5070/C64163843.

[SMKGS24b] David Smith, Joseph Samuel Myers, Craig S. Kaplan, and Chaim Goodman-Strauss. A chiral aperiodic monotile. *Combin. Theory*, 4(2):Paper No. 13, 2024. arXiv:2305.17743, doi:10.5070/C64264241.

[Soc89] J. E. S. Socolar. Simple octagonal and dodecagonal quasicrystals. *Phys. Rev. B*, 39(15):10519–10551, 1989. doi:10.1103/PhysRevB.39.10519.

[Soc90] J. E. S. Socolar. Weak matching rules for quasicrystals. *Comm. Math. Phys.*, 129(3):599–619, 1990. doi:10.1007/BF02097107.

[Soc23] J. E. S. Socolar. Quasicrystalline structure of the hat monotile tilings. *Phys. Rev. B*, 108(22):224109, 2023. doi:10.1103/PhysRevB.108.224109.

[Sta25] Jack Stade. Two tiling is undecidable. *arXiv e-prints*, 2025. arXiv:2506.11628.

[Tre23] Rodrigo Treviño. Aperiodic tilings, order, and randomness. *Notices Amer. Math. Soc.*, 70(8):1179–1191, 2023. doi:10.1090/noti2759.

[Was97] Lawrence C. Washington. *Introduction to Cyclotomic Fields*, volume 83 of *Graduate Texts in Mathematics*. Springer, New York, 2nd edition, 1997. doi:10.1007/978-1-4612-1934-7.

[WW23] James J. Walton and Michael F. Whittaker. An aperiodic tile with edge-to-edge orientational matching rules. *J. Inst. Math. Jussieu*, 22(4):1727–1755, 2023. doi:10.1017/S1474748021000517.

[WZ26] J. Washburn and M. Zlatanović. Uniqueness of the canonical reciprocal cost. *Mathematics*, 14(6):935, 2026. arXiv:2602.05753, doi:10.3390/math14060935.

[WZA26] J. Washburn, M. Zlatanović, and E. Allahyarov. The d'Alembert inevitability theorem. *Mathematics*, 14(8):1386, 2026. doi:10.3390/math14081386.